tively. Comparing the signal of each protein in HVJ-E with that before incorporation, we estimated incorporation efficiency of each protein into HVJ-E. Incorporation efficiency of Alexa488–BSA and OVA into HVJ-E was approximately 2.7 and 9.1%, respectively (data not shown). Consequently, 8.1 μg of Alexa488–BSA and 9.1 μg of OVA were delivered to the nasal cavities when the mice were treated with 3,000 HAU of HVJ-E/Alexa488–BSA and 1,000 HAU of HVJ-E/OVA, respectively.

In the intranasal treatment of healthy mice or AR model mice, 10 μl of HVJ-E/OVA, 10 μl of empty HVJ-E (total amount is 1,000 HAU) alone, 10 μl of OVA, 10 μl of a mixture of HVJ-E and OVA (MIX), and 10 μl of PBS (negative control) were administrated. In each case, 1,000 HAU of HVJ-E and 9.1 μg OVA were used.

Histological examination

Twenty-four hours after nasal challenge, the mice were anesthetized deeply and perfused from the left ventricle to the right atrium with 4% paraformaldehyde (PFA). Next, their heads were removed, fixed overnight with 4% PFA, and decalcified with 10% Na_4EDTA (EDTA, ethylenediaminetetraacetic acid) for 14 days. The nasal tissues were then cut into 10-μm coronal sections, stained with 4′,6-diamidino-2-phenylindole (DAPI), and observed under a fluorescence microscope.

AR model mice

BALB/c mice were immunized intraperitoneally with one injection per week for 3 weeks (weeks 0, 1, and 2) by injection with a mixture of 100 μl of OVA (1 μg/μl in PBS) and 100 μl of $Al(OH)_3$ (20 mg/ml, pH 7.5; Wako Pure Chemical Industries, Osaka, Japan) as an adjuvant, and 100 μg of OVA was administrated intranasally on week 2 based on the previous reports [25, 26].

Timeline of experiments using AR model mice

The experimental timeline is shown in Fig. 1. First, AR model mice were constructed. BALB/c mice were sensitized three times by intraperitoneal injection of OVA and alum and once by intranasal administration of OVA. Three weeks after the last sensitization, AR model mice were administrated with molecules (HVJ-E/OVA, HVJ-E, OVA, MIX, and PBS) once a week for 3 weeks. One week after the last therapeutic procedure, cytokines released from splenocytes were quantified by using enzyme-linked immunosorbent assay (ELISA). After the therapies, the mice were exposed to OVA. From 5 to 11 weeks after the first sensitization, blood was taken from the tail vein, and serum OVA-specific IgE was quantified by using ELISA.

Preparation of splenocytes

The mice were euthanized, and spleens were taken. The spleens were homogenized by using ground glasses in a Roswell Park Memorial Institute (RPMI) 1640 medium supplemented with 10% fetal bovine serum, 100 μg/ml streptomycin, and 100 U/ml penicillin. Splenocytes were homolyzed with the mixture of 4.5 ml of 0.83% NH_4Cl and 0.5 ml of 170 mM Tris–HCl (pH 7.65) for 5 min and washed twice with 10 ml of the medium.

Measurement of cytokine production by splenocytes

Murine splenocytes were seeded in 24-well plates (5.0×10^6 cells/well) in 1 ml of RPMI 1640 medium supplemented with 10% fetal bovine serum, 100 μg/ml streptomycin, and 100 U/ml penicillin. After a 96-h incubation in the presence or absence of OVA (50 μg/well) at 37°C in an atmosphere containing 5% CO_2, culture supernatants were harvested for measurement of IL-4, IL-5, and IFN-γ levels using ELISA kits (R&D Systems, Minneapolis, MN) according to the manufacturer's instructions.

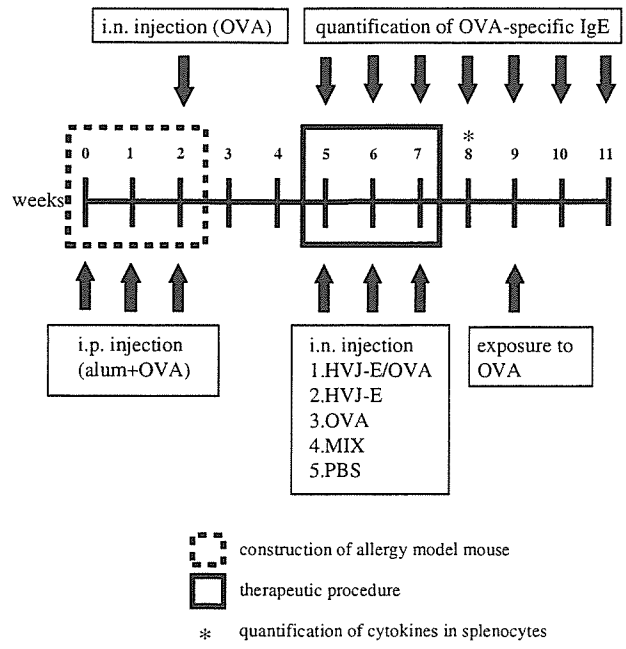

Fig. 1 Experimental timeline. Mice received intraperitoneal injection of OVA and alum for 3 weeks. Immediately after the last intraperitoneal injection, we administered OVA to the nasal cavities to induce AR. After 3 weeks, the mice were treated intranasally once per week for 3 weeks with HVJ-E/OVA, empty HVJ-E alone, OVA alone, MIX or PBS. Finally, the mice were exposed to allergen (OVA)

Quantification of OVA-specific serum IgE

Serum levels of OVA-specific IgE were quantified using a two-step sandwich ELISA. Plates (flat-bottomed 96-well; Becton Dickinson Labware, Franklin Lakes, NJ) were coated with purified anti-mouse IgE monoclonal antibody (2 μg/ml in PBS; PharMingen, San Diego, CA) at 37°C for 1 h. Subsequently, the plates were washed, blocked for 30 min at room temperature with 200 μl of 1% BSA in PBS, and washed three times with a washing buffer (0.05% Tween 20 in PBS). Serum samples were diluted in 1% BSA in PBS, added to the plates, and incubated for 1 h at room temperature. After washing three times with the washing buffer, the plates were incubated for 1 h at room temperature with OVA (10 μg/ml in 1% BSA in PBS). A detecting antibody (horseradish peroxidase-conjugated IgG

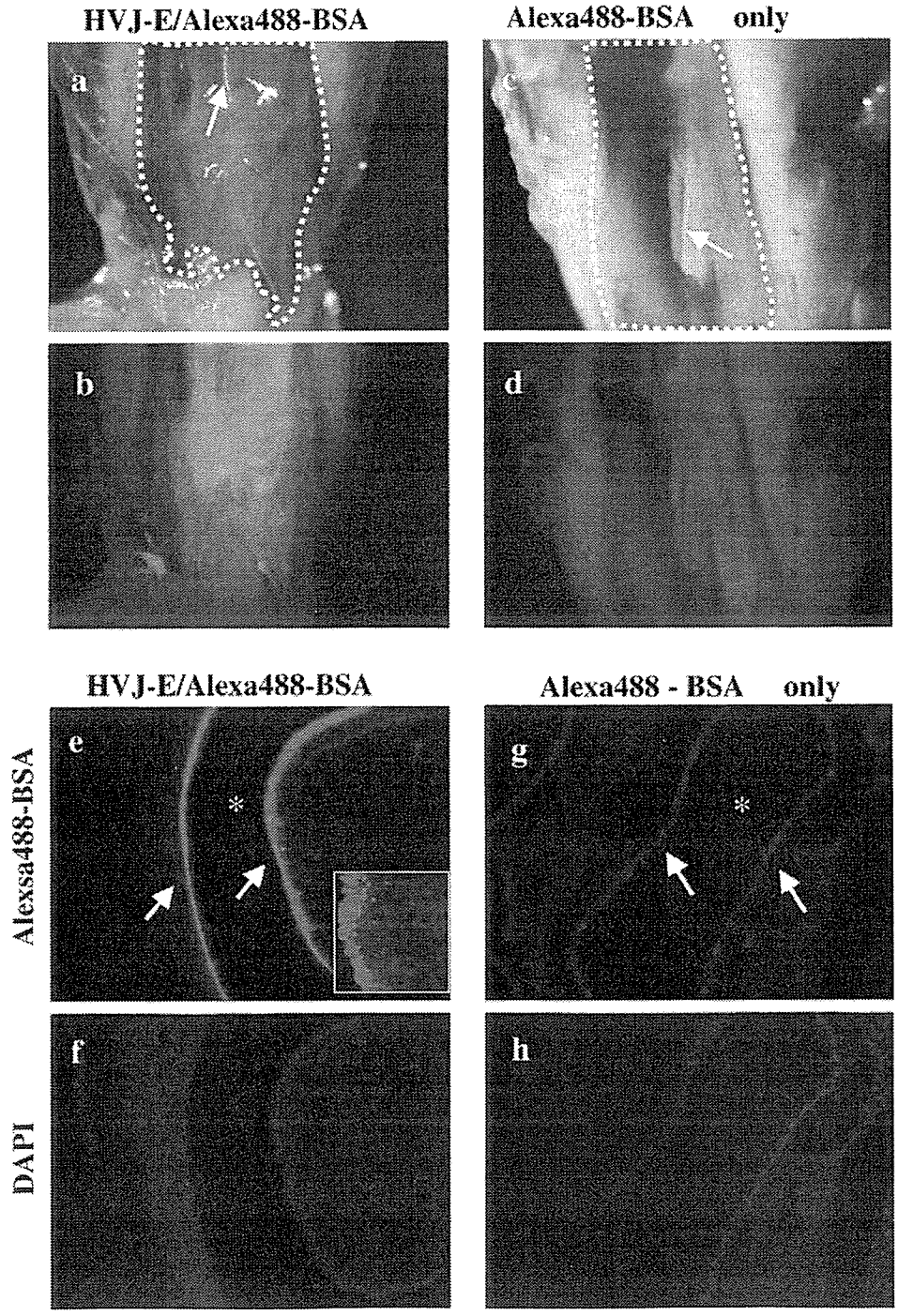

Fig. 2 Protein delivery to murine nasal mucosa using the HVJ-E system. Alexa488–BSA (*green*) was delivered to the murine nasal mucosa using HVJ-E (**a**, **b**, **e** and **f**) or without vector (**c**, **d**, **g** and **h**). (**b**) and (**d**) are fluorescence microscopic view of (**a**) and (**d**), respectively. *Arrows* in (**a**) and (**c**) indicate nasal septum; *arrows* in (**e**) and (**g**), nasal mucosa; *asterisks* in (**e**) and (**g**), nasal cavity. In (**f**) and (**h**), nuclei were stained with DAPI (*blue*). The *inset* in (**e**) shows a higher magnification merged view of the nasal epithelium after treatment with HVJ-E containing Alexa488–BSA. Original magnification, ×40 (**a**–**d**), ×400 (**e**–**h**), or ×1,000 (*inset* in **e**)

fraction of anti-OVA; Rockland, Gilbertsville, PA) was then added at a final dilution of 1:15,000. After incubating the plates for 30 min at room temperature, they were washed five times with the washing buffer. Finally, the plates were incubated for 15 min at room temperature with a substrate solution (ELISA POD Substrate TMB Kit Hyper; Nakalai Tesque, Kyoto, Japan) to allow color development. The reaction was terminated with a stop solution, and the absorbance at 450 nm in each well was measured with an ELISA plate reader (multi-plate reader Mithras LB940; Berthold Technologies, Wildbad, Germany). IgE levels were calculated as the fold increase over the plasma IgE level in the negative control mice.

Statistics

All results are expressed as means±standard error of mean. Data were compared using an unpaired Student's *t*-test for comparisons between the two groups and by analysis of variance followed by Dunnet's test for multiple comparisons. Differences were considered statistically significant when the *p* values were less than 0.05.

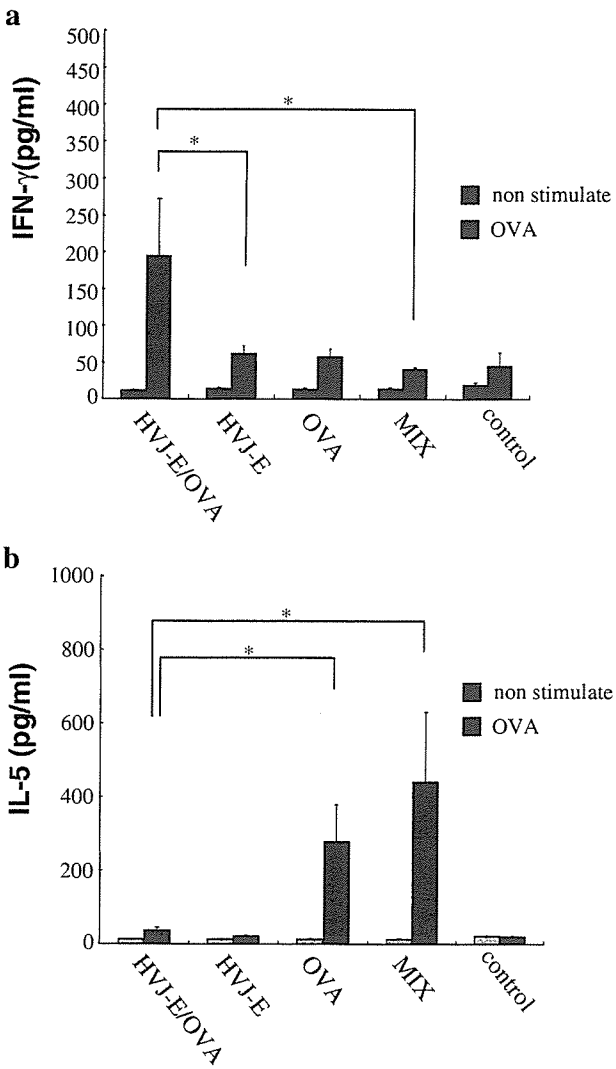

Fig. 3 Changes in the Th1/Th2 balance after intranasal sensitization in healthy mice. Expression of Th1/Th2 cytokines were examined in the mice (n=5 animals per group) receiving intranasal administration of HVJ-E/OVA, empty HVJ-E alone, OVA alone, MIX or PBS (negative control; n=5 animals per group) three times per week for 3 weeks. Splenocytes were isolated from the mice and incubated with or without OVA, after which, cytokine production was measured by ELISA. The HVJ-E/OVA group produced a higher level of IFN-γ (**a**) and lower level of IL-5 (**b**; *p<0.05). The OVA and MIX groups produced higher level of IL-5 (**b**; *p<0.05). The results are representative of three independent experiments

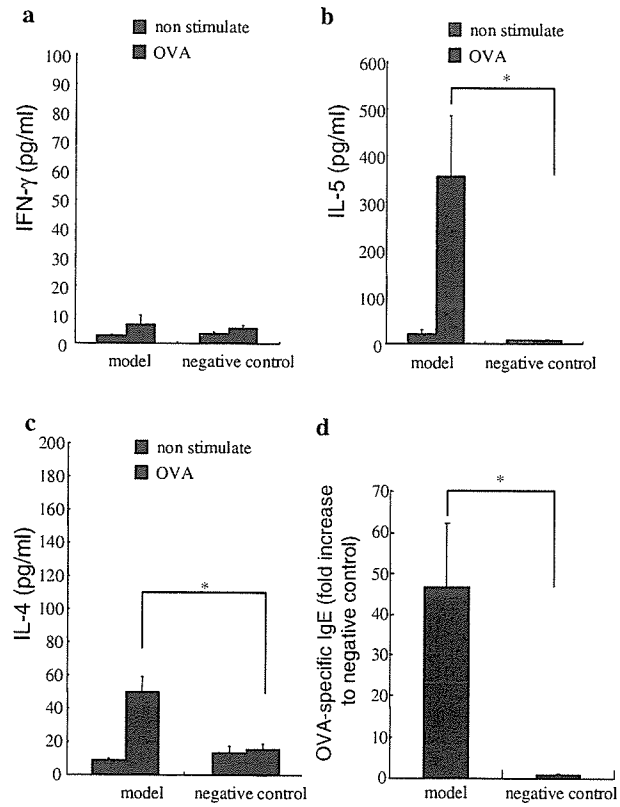

Fig. 4 Cytokines and IgE in AR model mice. Production of cytokines and IgE by splenocytes from AR model mice (n=5 animals per group). Compared to splenocytes from negative control mice, splenocytes from AR model mice produced higher levels of Th2 cytokines IL-4 (*p<0.01) and IL-5 (*p<0.05) and lower levels of the Th1 cytokine IFN-γ (**a**, **b** and **c**). AR model mice also produced exhibited serum levels of OVA-specific IgE (**d**; *p<0.05). The results are representative of three independent experiments

Results

Intranasal protein delivery using HVJ-E

We investigated whether protein could be efficiently introduced into the nasal mucosa without damage using the HVJ-E delivery system. We placed a 10-μl drop of 3,000 HAU of HVJ-E suspension containing BSA–Alexa Fluor®488 conjugate (HVJ-E/Alexa488–BSA) onto the nasal cavities of the mice using a micropipette, after which, all the mice inhaled the suspension. After 24 h, stereoscopic examination revealed fluorescence in the nasal mucosa of all mice treated with HVJ-E/Alexa488–BSA (Fig. 2a and b) but not in mice treated with Alexa488–BSA alone (Fig. 2c and d). Microscopic analysis of the coronal nasal sections confirmed that Alexa488–BSA was effectively incorporated into the nasal epithelium of mice treated with HVJ-E/Alexa488–BSA (Fig. 2e and f) but not with Alexa488–BSA alone (Fig. 2g and h). None of the treatments caused significant pathological changes in the nasal mucosa (data not shown).

Treatment with HVJ-E/OVA changes the Th1/Th2 balance in healthy BALB/c mice

To investigate the systemic immunological effect of allergen delivery to the nasal mucosa by HVJ-E, we analyzed changes in Th1/Th2 cytokine levels in splenocytes from healthy BALB/c mice. We sensitized BALB/c mice (n=5 per group) every week for 3 weeks (weeks 0, 1, and 2) by intranasal treatment with HVJ-E/OVA, empty HVJ-E alone, OVA alone, MIX, and PBS (negative control). On week 3, we isolated spleen from the mice, cultured the splenocytes with or without OVA for 96 h, and quantified cytokine production in each group using ELISA. After stimulation with OVA, splenocytes from the HVJ-E/OVA treatment group produced higher levels of IFN-γ and lower level of IL-5. In contrast, the OVA and MIX treatment groups produced higher levels of IL-5, although they did not produce significant levels of IFN-γ (Fig. 3).

Effect of administration of HVJ-E/OVA on cytokine release from splenocytes and plasma OVA-specific IgE levels in a mouse model of AR

To investigate the effect of HVJ-E/OVA treatment in a mouse model of AR, we first produced allergic BALB/c

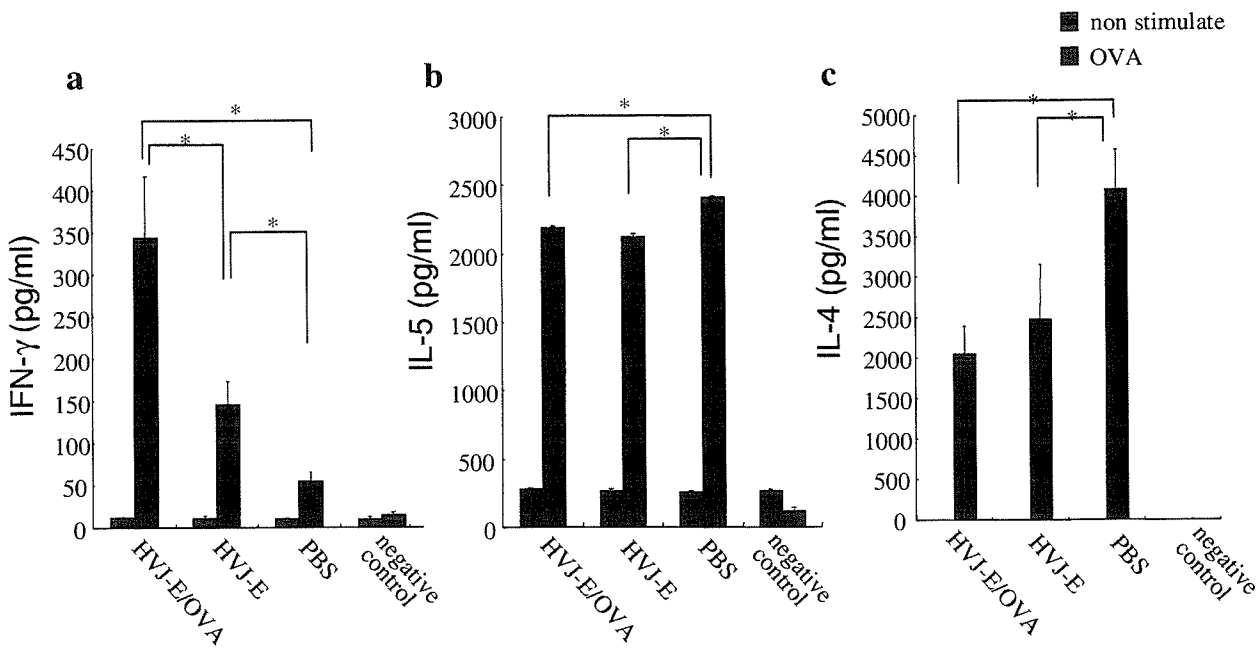

Fig. 5 Cytokine release from AR model splenocytes after intranasal administration of HVJ-E/OVA, HVJ-E, or PBS. Production of cytokines from splenocytes of AR model mice was measured by ELISA (n=5 animals per treatment group; n=3 for negative control). Splenocytes from mice treated with HVJ-E/OVA produced a higher level of IFN-γ than those from mice treated with HVJ-E or PBS. The empty HVJ-E group produced higher level of IFN-γ than the PBS group (**a**; *p<0.05). In addition, splenocytes from mice treated with HVJ-E/OVA or empty HVJ-E produced lower levels of IL-4 and IL-5 than those from mice treated with PBS (**b** and **c**; *p<0.05). The amount of IL-4 without stimulation was not detected in each sample. Negative control means the sample from healthy mice. The results are representative of two independent experiments

mice by immunization with OVA. Briefly, the mice were injected intraperitoneally with alum-precipitated OVA every week for 3 weeks (weeks 0, 1, and 2), and at the last week (at week 2), the mice were challenged intranasally with OVA (Fig. 1). One week after the last injection, we analyzed the Th1/Th2 balance and quantified serum OVA-specific IgE. In the AR model mice, splenocytes produced higher levels of IL-4 and IL-5 and lower levels of IFN-γ than the control mice (Fig. 4a–c). These results indicate the cytokine response to OVA was shifted to a Th2 response in the AR model mice, which is consistent with a type I allergic state. Furthermore, the level of serum OVA-specific IgE, which is a marker for allergy, was more than 40-fold higher in the AR model mice than the control mice (Fig. 4d).

We next examined the therapeutic effect of intranasal administration of HVJ-E/OVA. We quantified the cytokine production from splenocytes 1 week after the last treatment with HVJ-E/OVA in the AR model mice (n=5 animals per group). We also drew blood from the tail vein every week to measure the plasma OVA-specific IgE level in the AR model mice (n=5 animals per group) according to the protocol depicted in Fig. 1. Higher levels of IFN-γ were produced in response to OVA by splenocytes from mice treated with HVJ-E/OVA than mice treated with HVJ-E alone or PBS. The mice treated with empty HVJ-E produced higher level of IFN-γ than the mice treated with PBS (non-therapy; Fig. 5a). In addition, OVA induced lower levels of IL-4 and IL-5 in splenocytes from the mice treated with HVJ-E/OVA or HVJ-E than in splenocytes from the PBS-treated mice (Fig. 5b and c). Finally, we examined OVA-induced IgE production (Fig. 6). Significant levels of IgE were produced in response to OVA by the mice treated with empty HVJ-E or PBS (Fig. 6). The treatment with HVJ-E/OVA dramatically suppressed OVA-induced IgE production. The level of OVA-specific IgE did not increase after exposure to OVA at week 9. Three administrations of HVJ/OVA were necessary to obtain the results shown in Figs. 5 and 6. OVA-specific IgE levels of the MIX and OVA groups were elevated 6 weeks after the first sensitization and they were significantly (more than 20 times) higher than that of the HVJ-E/OVA group. The high IgE-level was maintained in both groups thereafter.

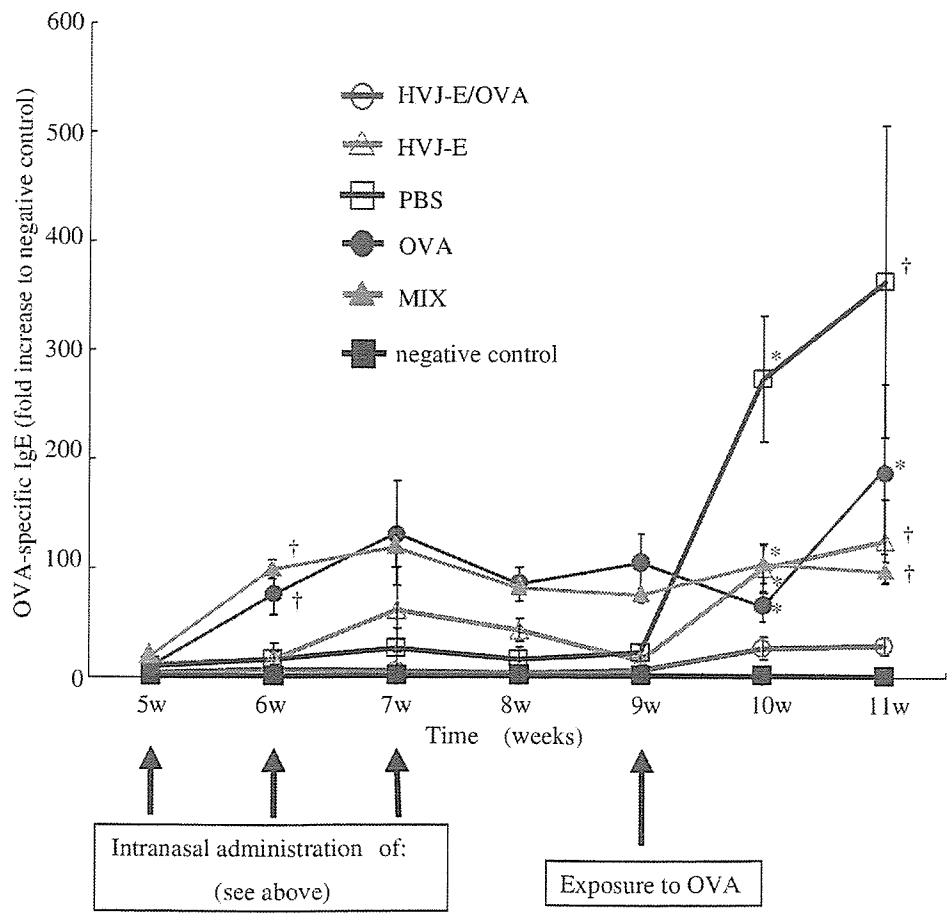

Fig. 6 Time course of the changes in the plasma level of OVA-specific IgE in AR model mice. The plasma level of OVA-specific IgE was monitored weekly in AR model mice (n=5 animals per group). Exposure to OVA (9 weeks after the first sensitization) enhanced the OVA-specific IgE level more than 100-fold compared to mice sensitized with HVJ-E or PBS. Mice sensitized with HVJ-E/OVA, however, produced significantly lower levels of OVA-specific IgE than mice sensitized with HVJ-E, OVA, MIX, or PBS (*p<0.05 and †p<0.01). The results are representative of three independent experiments

Discussion

Th2 immune response is characterized by the development of IL-4- and IL-5-producing effector T cells, which induce the production of IgE and promote development, maturation, and recruitment of eosinophils [27, 28]. The role of the cytokines IFN-γ and IL-4 in IgE regulation has been established [29, 30]. IFN-γ inhibits IgE production from B cells by suppressing Th2 cytokine release and reducing the expression of CD40-ligand on Th2 cells, which has an important role of Th2 cell–B cell contact [31, 32]. There are many examples of experimental models showing that suppression of Th2 response, including IgE production, can be manipulated by administration of recombinant cytokines (IL-12, IFN-γ) or cytokine antagonists (antagonists for IL-4 or IL-5) [33–35].

In this study, we showed that HVJ-E-mediated challenge with OVA enhances the OVA-induced production of IFN-γ from splenocytes in both healthy and AR model mice. Using the mouse model of AR, we also demonstrated in vivo that intranasal treatment with HVJ-E/OVA reduced the production of IL-4 and IL-5 by splenocytes and suppressed the elevation of serum IgE in response to OVA.

In our present study, both the OVA and MIX groups produced IL-5 in healthy mice (Fig. 3b). Previous report indicated that AR model mice could be established by only intranasal administration of OVA without need of intraperitoneal injection [36]. Therefore, it is likely that the mice in those groups were sensitized with OVA. Moreover, AR model mice treated with either OVA or MIX produced higher levels of OVA-specific IgE 6 weeks after the first sensitization, but they did not respond to after sensitizations (Fig. 6). Because continuous exposure to allergen induced tolerance to the allergen [37], both the OVA and MIX groups may have conducted tolerance to OVA in the AR model mice by repeated exposure to OVA (seven times in 9 weeks; Fig. 1). In spite of the presence of empty HVJ-E, cytokine release and IgE production of the MIX group were very similar to those of the OVA group (Figs. 3 and 6). The empty HVJ-E appeared to have minimum effect on these groups.

In this study, the production of IFN-γ in the HVJ-E group was significantly higher than the PBS group, and the production of Th2 cytokines were suppressed in the AR model mice (Fig. 5). Although the HVJ-E group (1,000 HAU of HVJ-E/head) did not enhance IFN-γ in healthy mice (Fig. 3), intranasal administration of larger amount of HVJ-E (3,000 HAU/head) could enhance IFN-γ in healthy mice (data not shown). It is well-known that live HVJ dramatically increases the production of type I IFNs [38, 39]. Even inactivated HVJ has the potential for producing type I IFNs, although the amount is much smaller compared with that by live HVJ [38, 40]. Type I IFN can induce the production of IFN-γ [41, 42]. From these facts, it is likely that HVJ-E itself has the potential to enhance IFN-γ production in mice that leads to the suppression of the Th2 response [28]. In our present study, the HVJ-E group (1,000 HAU/head) did not produce IFN-γ in healthy mice (Fig. 3a) but affected the Th1/Th2 cytokine balance in the AR model mice (Fig. 5a–c). In healthy mice, Th1/Th2 balance is well regulated because Th1 or Th2 can down-regulate each other [10, 11]. Previous report indicated that Th1/Th2 cytokine balance in allergy patients was more easily influenced by changes of circumstances in comparison with healthy individuals [43]. Therefore Th1/Th2 cytokine balance in the AR model mice might be more easily affected by HVJ-E treatment than that in healthy mice.

Previous studies indicate that exogenous proteins delivered to cells by fusogenic system are recognized as endogenous proteins because they are delivered into the cytoplasm directly and induce major histocompatibility complex class I antigen presenting pathway that activates cytotoxic T lymphocytes [44, 45] and enhances the production of IFN-γ from splenocytes [44]. In this study, OVA administrated to the nasal cavities by HVJ-E fusogenic system was delivered directly into the cytoplasm, recognized as an endogenous protein and primed effector T cells that produce IFN-γ against OVA. Therefore, IFN-γ produced from splenocytes might reduce Th2 cytokines and OVA-specific IgE production in the AR model mice.

In conclusion, HVJ-E/OVA might attenuate allergic response by the following reasons: HVJ-E itself may have the potential to enhance the production of IFN-γ, presumably, by stimulating dendritic cells [38, 40], and because OVA was directly delivered into the cytoplasm by the HVJ-E fusogenic system and recognized as an endogenous protein, IFN-γ production might be induced from effector T cells to suppress Th2 cytokines and OVA-specific IgE production [31, 32].

Although further investigation is needed to clarify the mechanism, it is evident that intranasal administration of HVJ-E containing an allergen is very effective for the systemic suppression of allergic responses. Therefore, in principle, this approach should be useful for the treatment of a variety of allergic disorders. Moreover, intranasal administration of HVJ-E is much less invasive than other injection methods. Using this needleless protein delivery system, it would be possible to deliver allergen to AR patients in a nasal spray similar to those used for nasal steroids. We are currently preparing clinical grade HVJ-E as described previously [46], and we hope that it will soon be available as a new clinical treatment of allergic diseases.

Acknowledgment This work was supported by a grant from the Ministry of Health, Labor, and Welfare of Japan.

References

1. Naclerio RM (1991) Allergic rhinitis. N Engl J Med 325:860–869
2. Savage J, Roy D (2005) Allergic rhinitis: an update. J R Soc Health 125:172–175
3. Platts-Mills TA (2001) The role of immunoglobulin E in allergy and asthma. Am J Respir Crit Care Med 164:S1–S5
4. Kitaura J, Song J, Tsai M, Asai K, Maeda-Yamamoto M, Mocsai A, Kawakami Y, Liu FT, Lowell CA, Barisas BG, Galli SJ, Kawakami T (2003) Evidence that IgE molecules mediate a spectrum of effects on mast cell survival and activation via aggregation of the FcεRI. Proc Natl Acad Sci U S A 100:12911–12916
5. Pandey V, Mihara S, Fensome-Green A, Bolsover S, Cockcroft S (2004) Monomeric IgE stimulates NFAT translocation into the nucleus, a rise in cytosol Ca^{2+}, degranulation, and membrane ruffling in the cultured rat basophilic leukemia-2H3 mast cell line. J Immunol 172:4048–4058
6. Bacharier LB, Geha RS (2000) Molecular mechanisms of IgE regulation. J Allergy Clin Immunol 105:S547–S558
7. Umetsu DT, DeKruyff RH (1997) Th1 and Th2 CD4+ cells in the pathogenesis of allergic diseases. Proc Soc Exp Biol Med 215:11–20
8. Grogan JL, Locksley RM (2002) T helper cell differentiation: on again, off again. Curr Opin Immunol 14:366–372
9. Szabo SJ, Kim ST, Costa GL, Zhang X, Fathman CG, Glimcher LH (2000) A novel transcription factor, T-bet, directs Th1 lineage commitment. Cell 100:655–669
10. O'Garra A (1998) Cytokines induce the development of functionally heterogeneous T helper cell subsets. Immunity 8:275–283
11. Paludan SR (1998) Interleukin-4 and interferon-gamma: the quintessence of a mutual antagonistic relationship. Scand J Immunol 48:459–468
12. Chretien I, Pene J, Briere F, De Waal Malefijt R, Rousset F, De Vries JE (1990) Regulation of human IgE synthesis. I. Human IgE synthesis in vitro is determined by the reciprocal antagonistic effects of interleukin 4 and interferon-gamma. Eur J Immunol 20:243–251
13. Purkerson J, Isakson P (1992) A two-signal model for regulation of immunoglobulin isotype switching. FASEB J 6:3245–3252
14. Romagnani S (1990) Regulation and deregulation of human IgE synthesis. Immunol Today 11:316–321
15. Snapper CM, Paul WE (1987) Interferon-gamma and B cell stimulatory factor-1 reciprocally regulate Ig isotype production. Science 236:944–947
16. Paul WE (1989) Pleiotropy and redundancy: T cell-derived lymphokines in the immune response. Cell 57:521–524
17. Stevens TL, Bossie A, Sanders VM, Fernandez-Botran R, Coffman RL, Mosmann TR, Vitetta ES (1988) Regulation of antibody isotype secretion by subsets of antigen-specific helper T cells. Nature 334:255–258
18. Finkelman FD, Katona IM, Urban JF, Jr., Holmes J, Ohara J, Tung AS, Sample JV, Paul WE (1988) IL-4 is required to generate and sustain in vivo IgE responses. J Immunol 141:2335–2341
19. Finkelman FD, Katona IM, Urban JF, Jr., Snapper CM, Ohara J, Paul WE (1986) Suppression of in vivo polyclonal IgE responses by monoclonal antibody to the lymphokine B-cell stimulatory factor 1. Proc Natl Acad Sci U S A 83:9675–9678
20. Kilmon MA, Ghirlando R, Strub MP, Beavil RL, Gould HJ, Conrad DH (2001) Regulation of IgE production requires oligomerization of CD23. J Immunol 167:3139–3145
21. von Garnier C, Astori M, Kettner A, Dufour N, Heusser C, Corradin G, Spertini F (2000) Allergen-derived long peptide immunotherapy down-regulates specific IgE response and protects from anaphylaxis. Eur J Immunol 30:1638–1645
22. Kaneda Y, Nakajima T, Nishikawa T, Yamamoto S, Ikegami H, Suzuki N, Nakamura H, Morishita R, Kotani H (2002) Hemagglutinating virus of Japan (HVJ) envelope vector as a versatile gene delivery system. Molec Ther 6:219–226
23. Okada Y (1993) Sendai virus-induced cell fusion. Methods Enzymol 221:18–41
24. Ito M, Yamamoto S, Nimura K, Hiraoka K, Tamai K, Kaneda Y (2005) Rad51 siRNA delivered by HVJ envelope vector enhances the anti-cancer effect of cisplatin. J Gene Med 7:1044–1052
25. Ikeda Y, Kaneko A, Yamamoto M, Ishige A, Sasaki H (2002) Possible involvement of suppression of Th2 differentiation in the anti-allergic effect of Sho-seiryu-to in mice. Jpn J Pharmacol 90:328–336
26. Sakaguchi M, Ikeda Y, Kido T, Yuzurihara M, Kase Y, Yamamoto M, Ishige A, Sasaki H (2002) Pharmacological characteristics of Ryokan-kyomi-shinge-nin-to, an antiallergic Kampo medicine. Biol Pharm Bull 25:1562–1565
27. Greenfeder S, Umland SP, Cuss FM, Chapman RW, Egan RW (2001) Th2 cytokines and asthma. The role of interleukin-5 in allergic eosinophilic disease. Respir Res 2:71–79
28. Kidd P (2003) Th1/Th2 balance: the hypothesis, its limitations, and implications for health and disease. Altern Med Rev 8:223–246
29. Mosmann TR, Cherwinski H, Bond MW, Giedlin MA, Coffman RL (1986) Two types of murine helper T cell clone. I. Definition according to profiles of lymphokine activities and secreted proteins. J Immunol 136:2348–2357
30. Romagnani S (1991) Human TH1 and TH2 subsets: doubt no more. Immunol Today 12:256–257
31. Gauchat JF, Aubry JP, Mazzei G, Life P, Jomotte T, Elson G, Bonnefoy JY (1993) Human CD40-ligand: molecular cloning, cellular distribution and regulation of expression by factors controlling IgE production. FEBS Lett 315:259–266
32. Worm M, Henz BM (1997) Molecular regulation of human IgE synthesis. J Mol Med 75:440–447
33. Gavett SH, O'Hearn DJ, Li X, Huang SK, Finkelman FD, Wills-Karp M (1995) Interleukin 12 inhibits antigen-induced airway hyperresponsiveness, inflammation, and Th2 cytokine expression in mice. J Exp Med 182:1527–1536
34. Kung TT, Stelts DM, Zurcher JA, Jones H, Umland SP, Egan RW, Kreutner W, Chapman RW (1995) Interferon-gamma and antibodies to interleukin-5 and interleukin-4 inhibit the pulmonary eosinophilia in allergic mice. Inflamm Res 44 Suppl 2: S185–S186
35. Wynn TA, Eltoum I, Oswald IP, Cheever AW, Sher A (1994) Endogenous interleukin 12 (IL-12) regulates granuloma formation induced by eggs of *Schistosoma mansoni* and exogenous IL-12 both inhibits and prophylactically immunizes against egg pathology. J Exp Med 179:1551–1561
36. McCusker C, Chicoine M, Hamid Q, Mazer B (2002) Site-specific sensitization in a murine model of allergic rhinitis: role of the upper airway in lower airways disease. J Allergy Clin Immunol 110:891–898
37. Schramm CM, Puddington L, Wu C, Guernsey L, Gharaee-Kermani M, Phan SH, Thrall RS (2004) Chronic inhaled ovalbumin exposure induces antigen-dependent but not antigen-specific inhalational tolerance in a murine model of allergic airway disease. Am J Pathol 164:295–304
38. Lopez CB, Garcia-Sastre A, Williams BR, Moran TM (2003) Type I interferon induction pathway, but not released interferon, participates in the maturation of dendritic cells induced by negative-strand RNA viruses. J Infect Dis 187:1126–1136
39. Lopez CB, Moltedo B, Alexopoulou L, Bonifaz L, Flavell RA, Moran TM (2004) TLR-independent induction of dendritic cell maturation and adaptive immunity by negative-strand RNA viruses. J Immunol 173:6882–6889

40. Ito T, Amakawa R, Inaba M, Hori T, Ota M, Nakamura K, Takebayashi M, Miyaji M, Yoshimura T, Inaba K, Fukuhara S (2004) Plasmacytoid dendritic cells regulate Th cell responses through OX40 ligand and type I IFNs. J Immunol 172:4253–4259
41. Brinkmann V, Geiger T, Alkan S, Heusser CH (1993) Interferon alpha increases the frequency of interferon gamma-producing human CD4+ T cells. J Exp Med 178:1655–1663
42. Van Weyenbergh J, MP PSilva, Bafica A, Cardoso S, Wietzerbin J, Barral-Netto M (2001) IFN-beta and TGF-beta differentially regulate IL-12 activity in human peripheral blood mononuclear cells. Immunol Lett 75:117–122
43. Hoglund CO, Axen J, Kemi C, Jernelov S, Grunewald J, Muller-Suur C, Smith Y, Gronneberg R, Eklund A, Stiema P, Lekander M (2006) Changes in immune regulation in response to examination stress in atopic and healthy individuals. Clin Exp Allergy 36:982–992
44. Bungener L, Huckriede A, de Mare A, de Vries-Idema J, Wilschut J, Daemen T (2005) Virosome-mediated delivery of protein antigens in vivo: efficient induction of class I MHC-restricted cytotoxic T lymphocyte activity. Vaccine 23:1232–1241
45. Nakanishi T, Hayashi A, Kunisawa J, Tsutsumi Y, Tanaka K, Yashiro-Ohtani Y, Nakanishi M, Fujiwara H, Hamaoka T, Mayumi T (2000) Fusogenic liposomes efficiently deliver exogenous antigen through the cytoplasm into the MHC class I processing pathway. Eur J Immunol 30:1740–1747
46. Kaneda Y, Yamamoto S, Nakajima T (2005) Development of HVJ envelope vector and its application to gene therapy. Adv Genet 53PA:307–332

Targeted chemotherapy against intraperitoneally disseminated colon carcinoma using a cationized gelatin–conjugated HVJ envelope vector

Hidetoshi Mima,[1,3] Seiji Yamamoto,[1] Makoto Ito,[1] Ryuji Tomoshige,[2] Yasuhiko Tabata,[2] Katsuto Tamai,[1] and Yasufumi Kaneda[1]

[1]Division of Gene Therapy Science, Graduate School of Medicine, Osaka University, Osaka, Japan; [2]Department of Biomaterials, Fields of Tissue Engineering Institute for Frontier Medical Sciences, Kyoto University, Kyoto, Japan; and [3]Department of Digestive and Cardiovascular Medicine, University of Tokushima Graduate School, Tokushima, Japan

Abstract

The hemagglutinating virus of Japan envelope (HVJ-E; Sendai virus) vector derived from inactivated HVJ particles can be used to deliver DNA, proteins, and drugs into cells both *in vitro* and *in vivo*. HVJ-E is capable of delivering bleomycin, an anticancer drug, to various cancer cell lines, thereby producing 300-fold greater cytotoxicity than administration of bleomycin alone. In a mouse model of peritoneally disseminated colon cancer, we injected HVJ-E containing the *luciferase* gene into the peritoneum. Unexpectedly, *luciferase* gene expression was not observed within the tumor deposits or any organs. However, when combined with cationized gelatin (CG), CG-HVJ-E produced a high level of *luciferase* gene expression primarily within the tumor deposits. Forty-eight hours after introducing colon cancer cells into the peritoneum of experimental mice, CG-HVJ-E with or without bleomycin was injected into the abdominal cavity. Following six injections of bleomycin-incorporated CG-HVJ-E, complete responses were observed in 40% of the mice examined. All of the mice that received either empty CG-HVJ-E or bleomycin alone died within 40 days of having cancer cells introduced into the peritoneum. When the mice with complete responses were rechallenged with colon cancer cells from the same cell line, no tumors developed. Thus, CG-HVJ-E may suppress peritoneal dissemination of cancer. [Mol Cancer Ther 2006;5(4):1021–8]

Received 9/2/05; revised 12/20/05; accepted 1/25/06.

Grant support: Ministry of Health, Labour, and Welfare of Japan.

The costs of publication of this article were defrayed in part by the payment of page charges. This article must therefore be hereby marked advertisement in accordance with 18 U.S.C. Section 1734 solely to indicate this fact.

Requests for reprints: Yasufumi Kaneda, Division of Gene Therapy Science, Graduate School of Medicine, Osaka University, 2-2 Yamada-oka, Suita, Osaka 565-0871, Japan.
E-mail: kaneday@gts.med.osaka-u.ac.jp

doi:10.1158/1535-7163.MCT-05-0352

Introduction

Although improved surgical, chemotherapy, and radiotherapy methods have been developed to treat patients with cancer, it remains difficult to eradicate cancer completely. In particular, metastatic cancer involving multiple foci and microscopic cancers are hard to treat, and prevention of recurrence remains a difficult problem in cancer therapy (1). Antitumor immunotherapy holds great promise; however, a number of obstacles have been encountered in the course of its development (2, 3). Although immunotherapy can reduce, delay, and sometimes prevent tumor recurrence, a number of tumors progress after developing mechanisms to avoid recognition and elimination by the immune system (4, 5). A number of studies suggest that both tumor regression and induction of antitumor immunity are indispensable for complete tumor eradication. For this reason, immunotherapy is often combined with other therapies, such as surgical resection, radiotherapy, and chemotherapy (6, 7). Drug delivery systems have the potential to overcome the problem of escape from immune recognition and to increase the efficiency of killing of unresectable tumors (8).

One important issue in drug delivery vectors is how to cross the cell membrane to introduce therapeutic molecules (9). There are several ways to bypass the cell membrane. Liposome-mediated delivery results in drug uptake by endocytosis or phagocytosis. However, this requires rapid penetration of the endosome or phagosome membrane by the foreign molecules before degradation (10). Viruses can enter cells; thus, viral vectors are capable of penetrating cell membranes (11). Adenovirus can escape from the endosome by disrupting the endosomal membrane with penton fibers (12). This capability has been used to enhance the efficiency of gene transfer using transferrin-polylysine-DNA complexes (13). Other viruses fuse with the cell membrane, thereby introducing their genomes into the cytoplasm. There are two different mechanisms of virus-cell fusion: pH dependent and pH independent. Influenza virus (14), Semliki Forest virus (15), and vesicular stomatitis virus (16) exhibit pH-dependent fusion, whereas hemagglutinating virus of Japan (HVJ, Sendai virus; ref. 17) and retrovirus (18) fuse with the cell membrane at both acidic and neutral pH. Viral fusion proteins have been identified, and synthetic vectors expressing viral fusion proteins can transfer foreign genes efficiently into the cytoplasm (19). We attempted to use the fusion capabilities of Sendai virus for drug delivery. First, we developed HVJ-liposomes, in which drug-incorporated liposomes were fused with inactivated Sendai virus (20). HVJ-liposomes are capable

of delivering genes and synthetic oligodeoxynucleotides into cells in various animal models (21). To further simplify drug delivery using HVJ-liposomes, we tried to develop a nonviral delivery system. Finally, we developed an HVJ envelope (HVJ-E) vector (22, 23). Using this system, macromolecules, such as plasmid DNA, RNA, synthetic oligonucleotides, proteins, and peptides, get incorporated into inactivated HVJ particles by treatment with a mild detergent and centrifugation, after which they can be delivered to cells *in vitro* and *in vivo*. To enhance drug delivery, we combined HVJ-E with cationized gelatin (CG; ref. 24). CG-conjugated HVJ-E (CG-HVJ-E) was still capable of fusion. In CT-26 cells, CG-HVJ-E–mediated *luciferase* gene expression was ~10 to 20 times greater than that achieved using HVJ-E without conjugation to a polymer. Furthermore, the stability of HVJ-E in fresh mouse serum was greatly enhanced by conjugation with CG.

Herein, we show that CG-HVJ-E is a very effective vehicle for delivering bleomycin to tumor cells after peritoneal dissemination. Multiple injections of CG-HVJ-E/bleomycin produced complete responses in 40% of the mice examined, all of which were further resistant to tumor rechallenge.

Materials and Methods

HVJ

HVJ was amplified in chorioallantoic fluid from 10- to 14-day-old chick eggs, after which it was purified by centrifugation and inactivated by UV irradiation (99 mJ/cm^2), as previously described (22). Inactivated virus cannot replicate, but its capacity for viral fusion remains intact.

Cell Culture

Human cancer cells and mouse colon cancer CT-26 cells were maintained in DMEM supplemented with 10% fetal bovine serum and antibiotics.

Preparation of HVJ-E/Bleomycin

Inactivated HVJ (1.8×10^{10} particles) was mixed with 60 μL of 5 or 40 mg/mL bleomycin and 2 μL of 3% Triton X-100, as previously described (22). After 15 minutes of incubation at 4°C, the suspension was washed with 500 μL of PBS (pH 7.4) and centrifuged (18,500 × *g*) for 15 minutes at 4°C. After this, the suspension was again washed twice with 500 μL of PBS to completely remove the detergent and any unincorporated bleomycin. After centrifugation, the HVJ-E/bleomycin was suspended in 180 μL of PBS.

Preparation of CG-HVJ-E/Bleomycin, Polymer-Conjugated HVJ-E, and CG/Bleomycin

Cationization of gelatin was done by introducing ethylene diamine into the carboxyl groups of low molecular weight gelatin (MW = 5,000), as previously described (24), and the mole-to-mole ratio of amino groups to carboxyl groups within the gelatin was 48.7. A 5-mg amount of CG was added to 300 μL of PBS containing 3×10^{10} particles of HVJ-E vector containing bleomycin. The solution was mixed by tapping several times. After this, the solution was incubated on ice for 30 minutes, during which it formed CG-conjugated HVJ-E vector containing bleomycin, which was purified by centrifugation. CG-conjugated (MW = 100,000), dextran-conjugated, and pullulan-conjugated HVJ-E vectors were prepared by mixing 5 mg of these polymers (25–27) with 3×10^{10} particles of HVJ-E vector containing the *luciferase* gene. For *in vivo* use, 1.5×10^{10} particles of polymer-conjugated HVJ-E vector was suspended in 500 μL of PBS. CG/bleomycin without HVJ-E was prepared by mixing 5 mg CG with 100 μL of 5 or 40 mg/mL bleomycin followed by centrifugation. CG-*luciferase* gene without HVJ-E vector was also prepared according to the previous method (25).

Quantification of Bleomycin in HVJ-E

A total of eight HVJ-E/bleomycin suspensions were prepared using eight different concentrations of bleomycin (0, 5, 10, 20, 30, 40, 50, and 100 mg/mL). Each HVJ-E/bleomycin suspension (200 μL) was dissolved in an equal volume of chloroform. After being vortexed and centrifuged (18,500 × *g* for 15 minutes at 4°C), the aqueous layer was recovered and added to 800 μL of PBS. The bleomycin content was assessed by high-performance liquid chromatography. Peaks representing bleomycin A2 and B2 at 245 nm were added, after which the concentration of bleomycin was determined from the standard curve. The efficacy of bleomycin inclusion into this vector was quantitatively measured with high-performance liquid chromatography. The amount of bleomycin in 1,000 HAU of HVJ-E/bleomycin was 0.18 μg when 5 mg/mL bleomycin was used, 0.41 μg with 10 mg/mL bleomycin, 0.84 μg with 20 mg/mL bleomycin, 1.12 μg with 30 mg/mL bleomycin, 1.32 μg with 40 mg/mL bleomycin, 1.34 μg with 50 mg/mL bleomycin, and 1.52 μg with 100 mg/mL bleomycin. Thus, the amount of bleomycin incorporated into the HVJ-E vector increased in proportion to the bleomycin concentration up to 40 mg/mL of bleomycin, at which a plateau was reached. Therefore, 40 mg/mL of bleomycin was used to prepare the HVJ-E/bleomycin used for the *in vivo* experiments.

In vitro Experiments

To perform *in vitro* transfection of HVJ-E/bleomycin, 5×10^4 CT-26 cells were seeded into six-well plates 1 day before transfection. Cells were maintained in DMEM (Nakalai Tesque, Kyoto, Japan) supplemented with 10% fetal bovine serum, penicillin (50 units/mL), and streptomycin (50 μg/mL) and incubated at 37°C in 5% CO_2. Tissue culture medium and supplements were purchased from Nakarai Tesque. HVJ-E/bleomycin was prepared with 5 or 40 mg/mL bleomycin. A 5-μL aliquot of 5 mg/mL protamine sulfate (Nakarai Tesque) and 500 μL of medium were added to 30 μL of HVJ-E/bleomycin (3×10^9 particles). This HVJ-E/bleomycin solution was added to each well after removal of the cell culture medium. HVJ-E alone and five different concentrations of bleomycin alone (0, 1, 10, 25, and 100 μg/mL) were then added to some of the wells. After 30 minutes of incubation, the medium was changed to fresh medium. After 2 days of incubation, the cells were counted with a Coulter particle counter (Beckman Coulter, Fullerton, CA).

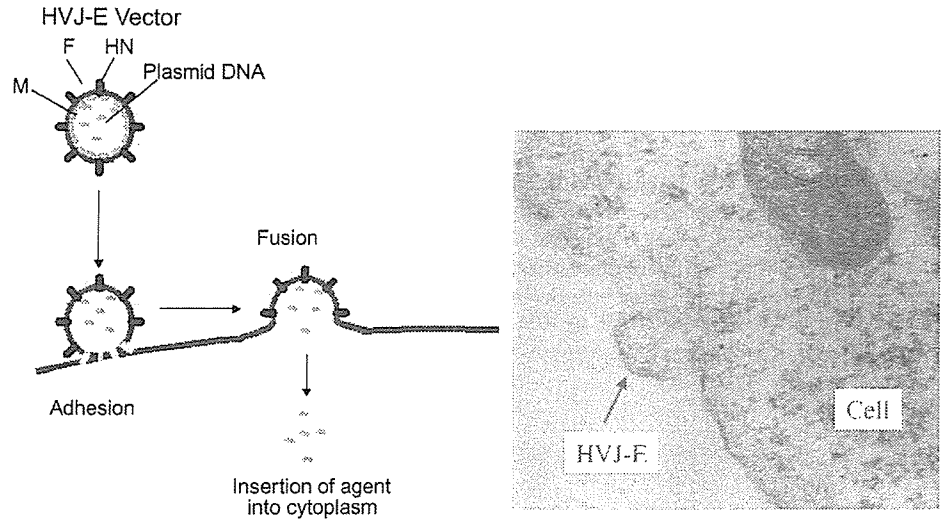

Figure 1. Schematic diagram and electron microscopy images of HVJ-E vector–mediated membrane fusion and drug delivery. The HVJ-E vector effectively encloses and delivers drugs into cells by membrane fusion.

Assessment of the Effect of Fusion and Endocytosis on HVJ-E and CG-HVJ-E Vector

For the evaluation of fusion-mediated delivery, we used antiserum against the F protein of HVJ prepared in our laboratory by immunizing a rabbit with purified F protein (24). The concentration of anti-F antibodies in the antiserum was ~30 μg/mL. Aliquots of antiserum were stored at −80°C. The antiserum was diluted with saline. HVJ-E (3×10^9 particles) and CG-HVJ-E containing the *luciferase* gene were preincubated with diluted or undiluted antiserum (20 μL) for 30 minutes at 37°C. This mixture was then added to cultured cells. Preimmune rabbit serum was used as the control. Luciferase activity was measured 24 hours after transfection.

To evaluate the effect of endocytosis-mediated delivery, wortmannin (Sigma Chemical Co., St. Louis, MO), an inhibitor of phosphatidylinositol-3-kinase that inhibits endocytosis (28), was used. The reagent was dissolved in DMSO to a final concentration of 10 mmol/L, dispensed into 5-μL aliquots, and stored at −80°C. Before use, the aliquots were thawed and diluted in serum-free DMEM. Care was taken to shield the aliquots from light. Before transfection, cells were washed with serum-free DMEM and incubated with various concentrations of wortmannin for 15 minutes. The cells were then subjected to *in vitro* transfection, as described above.

In vivo Experiments

All animal experiments were approved by the Animal Committee of Osaka University and conducted in a humane fashion according to their guidelines. Male BALB/c mice, 6 to 7 weeks of age, were obtained from Charles River Japan, Inc. (Yokohama, Japan). Mice were housed for 7 to 14 days and allowed *ad libitum* access to food and water. For tumor cell implantation, CT-26 cells were enzymatically detached from their culture flasks and counted. Viable cells (1.5×10^6) were resuspended in 500 μL of PBS and injected into the peritoneal cavity of each mouse. Two days after tumor inoculation, 500 μL of CG-HVJ-E/bleomycin (1.5×10^{10} particles) or CG-bleomycin were injected six times every third day, and animal survival was monitored.

Rechallenge Experiment

On day 115 after tumor inoculation, two surviving mice and three age-matched naive mice were rechallenged by i.d. injection of 5×10^6 parental cells into both sides of their trunk. In addition, two other surviving mice from the same experiment were rechallenged by i.p. injection of 1.5×10^6 parental cells.

Results

HVJ-E Vector Delivers Molecular Agents into Cells

The HVJ-E vector delivers molecules, such as anticancer drugs, into cells by membrane fusion, as illustrated in Fig. 1. We investigated the delivery mechanism using anti-F antibody or wortmannin. As shown in Supplementary Fig. S1A and B,[4] undiluted anti-F antibody reduced the transfection efficiency of HVJ-E to 20% of that of the control group, whereas 100 nmol/L wortmannin did not significantly decrease transfection efficiency. These results suggest that drug delivery by HVJ-E vector occurs mainly by fusion. Therefore, agents delivered by the HVJ-E vector are released directly into the cytoplasm, bypassing endocytosis, the mechanism by which liposome-mediated and naked DNA-mediated delivery are achieved.

HVJ-E Vector Enables Effective Delivery of Bleomycin into Cells

We attempted to incorporate anticancer drugs into the HVJ-E vector to enhance its cytotoxicity following fusion-mediated delivery. We used bleomycin as the anticancer agent to be incorporated into HVJ-E. Bleomycin has a

[4] Supplementary material for this article is available at Molecular Cancer Therapeutics Online (http://mct.aacrjournals.org/).

marked antineoplastic effect but limited cell permeability (29). To evaluate the potential of the HVJ-E vector to effectively deliver bleomycin into cancer cells, we incorporated bleomycin into the vector and assessed its cytotoxicity against various cancer cell lines *in vitro*. We prepared HVJ-E/bleomycin using 5 or 40 mg/mL of bleomycin in the HVJ-E inclusion reaction and tested its cytotoxicity against CT-26 mouse colon adenocarcinoma cells. HVJ-E/bleomycin or bleomycin alone were incubated with cultured cells for 30 minutes, and the cells were further cultivated for 48 hours. Bleomycin alone was not particularly cytotoxic, killing only 60% of CT-26 cells at 100 μg/mL of BML. Although HVJ-E alone was not toxic to CT-26 cells, HVJ-E/bleomycin killed >90% of CT-26 cells in the culture (Fig. 2A). The bleomycin content of HVJ-E/bleomycin prepared using 5 and 40 mg/mL of bleomycin in the inclusion reaction was 0.36 and 2.54 μg/mL, respectively. Therefore, HVJ-E/bleomycin was 300-fold more cytotoxic than bleomycin alone. HVJ-E/bleomycin exhibited similar effects on a number of other human cancer cell lines (Fig. 2B). Although the cytotoxicity of 100 μg/mL bleomycin varied among different human cancer cell lines, HVJ-E/bleomycin caused a marked reduction in cell survival in all cell lines tested. In addition, treatment with HVJ-E/bleomycin reduced the proportion of cells in the G_0-G_1 phase of the cell cycle and increased the proportion of cells in the G_2-M phase (data not shown). These cell cycle changes are a characteristic of bleomycin treatment. Thus, it seems that the HVJ-E vector efficiently delivered bleomycin into cells by fusion with the plasma membrane.

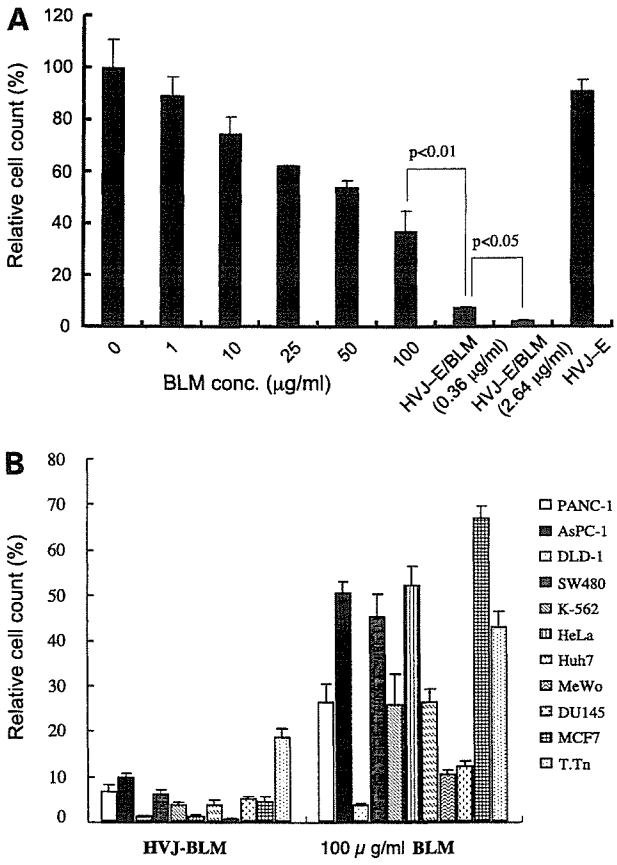

Figure 2. Efficient delivery of an antitumor agent (bleomycin, *BLM*) into cancer cells using the HVJ-E vector. **A**, after 30 min of HVJ-E/bleomycin transfection, cells were cultured for 2 d. After this, viable CT-26 cells were counted. When HVJ-E/bleomycin (5 and 40 mg/mL) was used, the concentration of bleomycin in the medium was 0.36 and 2.64 μg/mL, respectively. HVJ-E/bleomycin (5 mg/mL) significantly suppressed cell viability compared with bleomycin alone ($P < 0.01$). HVJ-bleomycin (40 mg/mL) also showed significantly higher cytotoxicity than HVJ-bleomycin (5 mg/mL; $P < 0.05$). **B**, investigation of HVJ-E/bleomycin cytotoxicity against various human cancer cell lines. PANC-1, pancreatic cancer; AsPC-1, pancreatic cancer; DLD-1, colon adenocarcinoma; SW480, colon cancer; K562, erythroleukemia; HeLa, uterocervical cancer; Huh-7, hepatocellular carcinoma; MeWo, malignant melanoma; DU145, prostate cancer; MCF7, mammary carcinoma; T.Tn, esophageal squamous cell carcinoma. In all tumor cells, HVJ-E/bleomycin showed significantly higher cytotoxicity compared with bleomycin alone ($P < 0.01$).

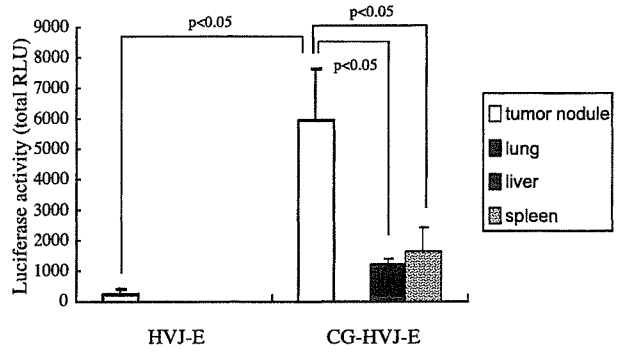

Figure 3. Luciferase expression in tumor nodules, liver, spleen and lung, following i.p. injection of HVJ-E or CG-HVJ-E containing the *luciferase* gene. Seven days after i.p. injection of CT-26 cells, HVJ-E or CG-HVJ-E containing the *luciferase* gene were injected into the peritoneal cavities of tumor-bearing mice. Luciferase activity in various organs was investigated 24 h after gene transfer. Significantly higher luciferase activity was obtained in tumor nodules using CG-HVJ-E than using HVJ-E alone ($P < 0.05$). Using CG-HVJ-E, luciferase activity was significantly higher in tumor nodules than in other organs ($P < 0.05$).

In vivo Gene Transduction for the Treatment of Peritoneally Disseminated Tumors

A major challenge in cancer chemotherapy is finding a way to treat inoperable and invisible cancer lesions and hence the need for cancer-specific drug delivery vectors. Here, we attempted to treat peritoneal deposits of cancer cells using the HVJ-E vector system. First, we confirmed the presence of peritoneal tumor deposits 1 week after i.p. injection of CT-26 tumor cells (10^7 cells). As previously reported (30), a number of tumor deposits are observed to develop within the i.p. cavity following the introduction of CT-26 tumor cells. In particular, metastasis to lymph nodes around the root of the mesentery are frequently detected in the i.p. cavity.

We used the *luciferase* gene as a reporter gene to measure gene expression. To evaluate the transfection efficiency of HVJ-E into peritoneally disseminated colon tumor cells, HVJ-E containing pcLuc plasmid was injected into the peritoneal cavities of mice 7 days after i.p.

injection of CT-26 tumor cells. Twenty-four hours after injection of HVJ-E, the mice were killed, and all tumor deposits and nonaffected organs were removed and examined for luciferase activity. As shown in Fig. 3, *luciferase* gene expression was not detected in either the tumor deposits or other organs, such as the lung, liver, or spleen. No significant luciferase activity was detected in any tissue when either naked plasmid DNA encoding the *luciferase* gene or CG-conjugated *luciferase* gene was i.p. injected (data not shown).

Next, we combined HVJ-E with CG (MW = 5,000 and 100,000), dextran, and pullulan. When CG (MW = 5,000)-HVJ-E containing the *luciferase* gene was i.p. injected, a high level of expression of the *luciferase* gene was preferentially detected in the tumor deposits compared with other polymers, such as CG (MW = 100,000), dextran, and pullulan, with limited expression in the spleen and liver and no expression in lung (Supplementary Fig. S2).[4]

Treatment of Peritoneally Disseminated Colon Cancer Using CG-HVJ-E/Bleomycin

Then, we combined HVJ-E containing bleomycin with CG (CG-HVJ-E/bleomycin) and compared its cytotoxicity against cultured CT-26 cells with that of HVJ-E/bleomycin. As shown in Fig. 4, CG-HVJ-E/bleomycin killed CT-26 cells as efficiently as HVJ-E/bleomycin. No cytotoxicity was observed when CG was combined with bleomycin alone (CG/bleomycin). We then investigated the mechanism of CG-HVJ-E–mediated delivery using anti-F antibody or wortmannin. As shown in Supplementary Fig. S3A and B,[4] both undiluted anti-F antibody and 100 nmol/L wortmannin significantly reduced the transfection efficiency of CG-HVJ-E. Thus, the delivery mechanism of CG-HVJ-E vector seems to depend on both membrane fusion and endocytotic uptake.

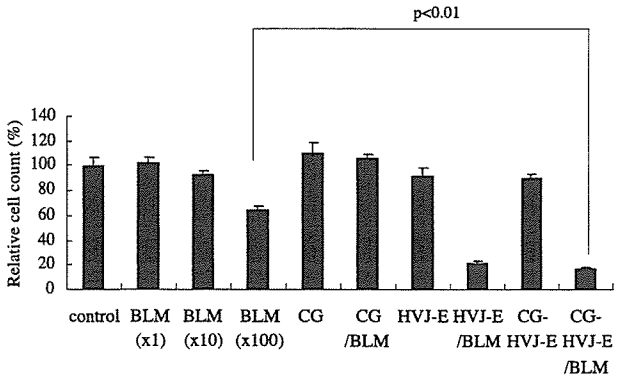

Figure 4. Cytotoxic effects of bleomycin (*BLM*) against CT-26 cells delivered by CG, HVJ-E or CG-HVJ-E. The concentration of bleomycin in (×1), (×10), (×100), CG/bleomycin, HVJ-E/bleomycin, and CG-HVJ-E/bleomycin was 0.36, 3.6, 36, 0.36, 0.36, and 0.36 μg/mL, respectively. Following 30 min of vector treatment, CT-26 cells were cultured for 2 d. After this, viable CT-26 cells were counted. As a control, cell viability without treatment was also evaluated. Significant cytotoxicity was obtained using CG-HVJ-E/bleomycin compared with bleomycin (×100) alone ($P < 0.01$). No significant differences in cytotoxicity were seen between CG-HVJ-E/bleomycin and HVJ-E/bleomycin.

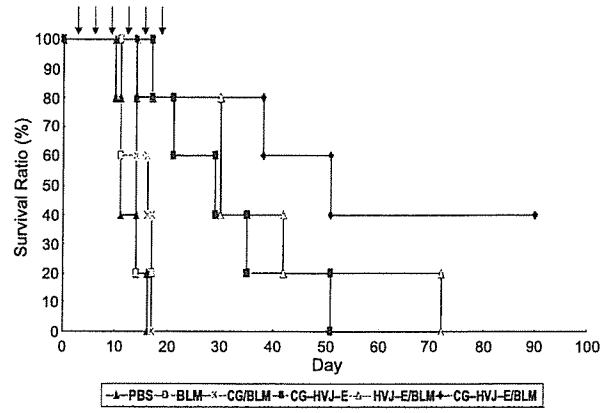

Figure 5. Survival of tumor-bearing mice. Two days after i.p. injection of CT-26 cells, CG or CG-HVJ-E containing bleomycin (*BLM*) was i.p. injected six times every third day. An empty vector without bleomycin, bleomycin alone, or PBS were also i.p. injected in a similar manner. The survival of tumor-bearing mice was monitored. Arrows indicate the timing of i.p. injection (on days 2, 5, 8, 11, 14, and 17) after tumor inoculation.

Next, we injected CG-HVJ-E/bleomycin into the peritoneal cavity 48 hours after the introduction of CT-26 cells. Three injections were given every third day. Although mouse survival was prolonged by administration of either CG-HVJ-E or CG-HVJ-E/bleomycin, compared with bleomycin alone, all of the mice died within 40 days (data not shown). Next, we evaluated the effects of i.p. injection of the vectors six times every third day. As shown in Fig. 5, complete responses were observed in 40% of the mice injected with CG-HVJ-E/bleomycin. The mice that received CG-HVJ-E without bleomycin showed prolonged survival, compared with those administered bleomycin alone, but still died within 50 days. The mice showing complete responses survived >90 days and experienced complete remission.

Rechallenge of Surviving Mice with CT-26

Next, we injected CT-26 cells into the surviving mice i.d. or i.p. Approximately 5×10^6 CT-26 cells were i.d. injected into both sides of the mouse trunk. Although the tumor masses were observed to grow up to 3 to 4 mm in diameter within 5 days of the rechallenge in both control mice and those showing complete responses, tumor masses among the mice previously showing complete responses then underwent a rapid reduction in size within 11 days of the rechallenge (Fig. 6). However, tumor masses among the control mice continued to grow up to 8 to 10 mm in diameter within 11 days of the rechallenge (Fig. 6). In addition, $\sim 1.5 \times 10^6$ CT-26 cells were also injected directly into the i.p. cavities of mice showing complete responses, as well as control mice. Within 11 days of the rechallenge, control mice were emaciated and had diarrhea, and a number of tumor deposits were observed in the peritoneal cavity, whereas the mice previously showing complete responses remained healthy with no tumor deposits observed within the peritoneal cavity (data not shown).

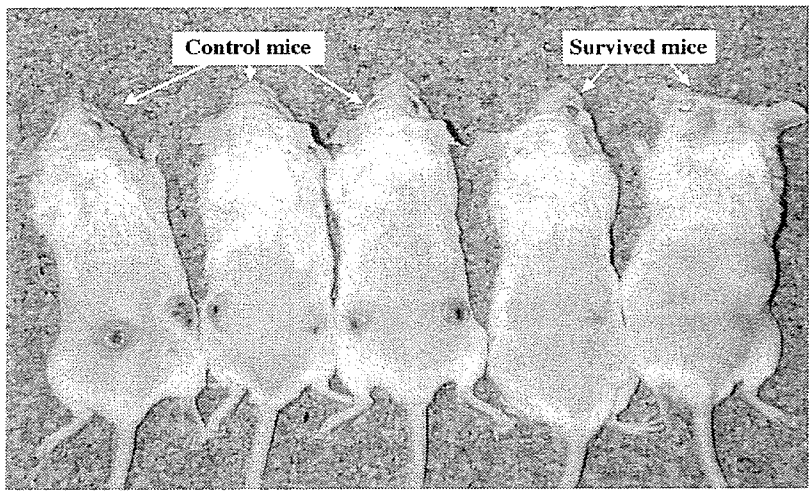

Figure 6. Resistance to rechallenge with parental CT-26 cells among mice previously showing complete responses. The two on the right previously treated with CG-HVJ-E/bleomycin (*BLM*) were rechallenged with i.d. injection of 5×10^6 parental CT-26 cells into both sides of the mouse trunk 115 d after initial tumor inoculation. The three mice on the left are age-matched naive mice. Within 11 d of tumor rechallenge, intradermal tumor formation was observed in each mouse.

However, when Meth-A cells, which are fibrosarcoma cells derived from BALB/c mouse, were i.d. injected into the surviving mice, tumors arose in those mice as well as in naive mice (data not shown).

Thus, multiple i.p. injection of CG-HVJ-E/bleomycin not only inhibits the tumorigenesis of CT-26 cells following i.p. dissemination but also induces an effective and long-lasting anti-CT-26 memory in mice.

Discussion

In this study, we showed the feasibility of using the HVJ-E vector for cancer treatment. One of the advantages of the HVJ-E vector is fusion-mediated drug delivery and thereby enhancing drug efficacy. Bleomycin is ~1,500 Da and thus has limited permeability into cells and low bioavailability following oral, i.m., or i.v. administration (29). In the present study, *in vivo*, cell culture experiments showed enhanced cytotoxicity of bleomycin delivered by the HVJ-E vector against a variety of cancer cells. Fusion between the HVJ-E vector and cancer cell membranes might overcome the problem of limited bleomycin cell permeability. As shown in Supplementary Fig. S3,[4] the delivery by CG-HVJ-E was mediated by both fusion and endocytosis. CG-HVJ-E may be more effective for drug delivery than HVJ-E alone because HVJ can fuse with the cell membrane under neutral conditions and also with the endosomal membrane under acidic conditions (17).

A disadvantage of the HVJ-E vector is rapid degradation in the presence of fresh serum, although the *in vitro* transfection efficiency of HVJ-E was not inhibited by culture medium containing 10% fetal bovine serum (22). However, we previously showed that CG-HVJ-E is remarkably stable in 50% fresh mouse serum. Although it is unproven that HVJ is degraded by complement lysis in mouse serum, as known to be the case for retrovirus and HIV (31, 32), the interaction between serum proteins and HVJ-E may contribute to reduced transfection efficacy of HVJ-E. Conjugation with CG seems to protect the surface molecules of HVJ-E from the detrimental effects of serum proteins (24). In this report, CG-HVJ-E showed a proclivity toward i.p. tumor deposits. In a previous report, we showed that HVJ-cationic liposomes also have a proclivity for tumor deposits when injected into peritoneal cavity (30). We speculate that HVJ-cationic liposomes might be absorbed into lymph vessels and fuse with tumor cells when they reach lymph nodes enlarged with tumor cells. We observed enhanced fusion of HVJ with tumor cells than normal cells.[5] Therefore, it is likely that positively charged CG-HVJ-E (ζ potential = 11.30 mV; ref. 24) results in preferential delivery of bleomycin to tumor cells within the peritoneum.

Another advantage of the HVJ-E vector is its capacity for repeated injection. Gene transfer to mouse muscle was not inhibited by repeated injections (23). Similar results were obtained when HVJ-liposomes was repeatedly injected into rat liver. After repeated injections, the anti-HVJ antibodies generated in mice were not sufficient to neutralize HVJ-liposomes (33). Presumably, this is because fusion occurs more rapidly than recognition by neutralizing antibodies. Indeed, fusion between the HVJ-E vector and the cell membrane occurs in 10 seconds (23).

In this experiment, complete responses were observed in 40% of tumor-inoculated mice. Furthermore, these mice were resistant against tumor rechallenge. This result indicates that antitumor immunity was achieved in mice treated with CG-HVJ-E/bleomycin. Some reports suggest that antitumor immunity might be induced in mice following a variety of forms of treatment, including chemotherapy, radiotherapy, or gene therapy (34–36). On the other hand, it is well known that viruses and bacteria can induce robust and long-lasting immune responses through Toll-like receptors (37, 38). Some

[5] Y. Kaneda, unpublished data.

reports suggest that live HVJ infection induces the secretion of various cytokines, including IFN-α, IFN-β, IFN-γ, interleukin-6, interleukin-12, and tumor necrosis factor in dendritic cells, while also inducing a maturation of dendritic cells (39, 40). Moreover, inactivated HVJ can induce dendritic cell maturation as effectively as live HVJ (39, 41). We observed a retained capability of dendritic cell maturation by the HVJ-E vector, and i.t. injection of the HVJ-E vector into mice mildly enhanced IFN-γ and interleukin-5 production by antigen stimulated splenocytes.[6] This explains why CG-HVJ-E prolonged mouse survival even without bleomycin. When rechallenged with tumor cells, the mice treated with CG-HVJ-E/bleomycin rejected the same CT-26 tumor not Meth-A. This suggests that tumor-specific cytotoxic T cells, not natural killer cells, were generated in those mice by CG-HVJ-E/bleomycin treatment. Therefore, CG-HVJ-E/bleomycin might induce antitumor immunity and via direct toxicity to tumor cells by bleomycin delivery. Given its dual function, the HVJ-E vector might be especially useful for tumor eradication. Currently, no drug delivery system has shown similar capabilities specific to the treatment of cancer.

Thus, the HVJ-E vector system shows potential for the treatment of cancer in the future.

References

1. McMillan TJ, Hart IR. Can cancer chemotherapy enhance the malignant behavior of tumours? Cancer Metastasis Rev 1987;6:503 – 19.

2. Steinman RM, Mellman I. Immunotherapy: bewitched, bothered, and bewildered no more. Science 2004;305:197 – 200.

3. Blattman JN, Greenberg PD. Cancer immunotherapy: a treatment for the masses. Science 2004;305:200 – 5.

4. Pawelec G. Immunotherapy and immunoselection: tumour escape as the final hurdle. FEBS Lett 2004;567:63 – 6.

5. Ahmad M, Rees RC, Ali SA. Escape from immunotherapy: possible mechanisms that influence tumor regression/progression. Cancer Immunol Immunother 2004;53:844 – 54.

6. Gardini A, Ercolani G, Riccobon A, et al. Adjuvant, adoptive immunotherapy with tumor infiltrating lymphocytes plus interleukin-2 after radical hepatic resection for colorectal liver metastases: 5-year analysis. J Surg Oncol 2004;87:46 – 52.

7. Smith RE, Colangelo L, Wieand HS, Begovic M, Wolmark N. Randomized trial of adjuvant therapy in colon carcinoma: 10-year results of NSABP protocol C-01. J Natl Cancer Inst 2004;96:1128 – 32.

8. Alen TM, Cullis PR. Drug delivery systems; entering the mainstream. Science 2004;303:1818 – 22.

9. Kaneda Y. Biological barriers to gene transfer. In: Amiji MM, editor. Polymeric gene delivery principles and application. Washington (DC): CRC Press; 2005. p. 29 – 41.

10. Wattiaux R, Laurent N, Wattiaux-De Coninck S, Jadot M. Endosomes, lysosomes: their implication in gene transfer. Adv Drug Deliv Rev 2000; 41:201 – 8.

11. Flint SJ, Enquist LW, Krug RM, Racaniello VR, Skalka AM, editors. Principles of virology. Washington (DC): ASM Press; 2000.

12. Seth P. Mechanism of adenovirus-mediated endosome lysis: role of the intact adenovirus capsid structure. Biochem Biophys Res Commun 1994;205:1318 – 24.

13. Wagner E, Zatloukal K, Cotten M, et al. Coupling of adenovirus to transferrin-polylysine/DNA complexes greatly enhances receptor-mediated gene delivery and expression of transfected genes. Proc Natl Acad Sci U S A 1992;89:6099 – 103.

14. Maeda T, Ohnishi S. Activation of influenza virus by acidic media causes hemolysis and fusion of erythrocytes. FEBS Lett 1980;122: 283 – 7.

15. Marsh M, Bolzau E, Helenius A. Penetration of Semliki Forest virus from acidic prelysosomal vacuoles. Cell 1983;32:931 – 40.

16. Blumenthal R, Bali-Puri A, Walter A, Covell D, Eidelman O. pH-dependent fusion of vesicular stomatitis virus with Vero cells. Measurement by dequenching of octadecyl rhodamine fluorescence. J Biol Chem 1987;262:13614 – 9.

17. Okada Y. Sendai virus-induced cell fusion. In: Duzgunes N, editor. Methods in enzymology. Vol. 221. San Diego: Academic Press Inc.; 1993. p. 18 – 41.

18. McClure MO, Sommerfelt MA, Marsh M, Weiss RA. The pH independence of mammalian retrovirus infection. J Gen Virol 1990;71: 767 – 73.

19. Wagner E, Plank C, Zatloukal K, Cotten M, Birnstiel ML. Influenza virus hemagglutinin HA-2 N-terminal fusogenic peptides augment gene transfer by transferrin-polylysine-DNA complexes: toward a synthetic virus-like gene-transfer vehicle. Proc Natl Acad Sci U S A 1992;89: 7934 – 8.

20. Saeki Y, Matsumoto N, Nakano Y, Mori M, Awai K, Kaneda Y. Development and characterization of cationic liposomes conjugated with HVJ (Sendai virus): reciprocal effect of cationic lipid for *in vitro* and *in vivo* gene transfer. Hum Gene Ther 1997;8:2133 – 41.

21. Kaneda Y, Saeki Y, Morishita R. Gene therapy using HVJ-liposomes: the best of both worlds? Mol Med Today 1999;5:298 – 303.

22. Kaneda Y, Nakajima T, Nishikawa T, et al. Hemagglutinating virus of Japan (HVJ) envelope vector as a versatile gene delivery system. Mol Ther 2002;6:219 – 26.

23. Kaneda Y, Yamamoto S, Nakajima T. HVJ envelope vector and its application to gene therapy. In: Huang L, Hung M-C, Wagner E, editors. Non-viral vectors for gene therapy. San Diego: Elsevier; 2005. p. 307 – 32.

24. Mima H, Tomoshige R, Kanamori T, et al. Biocompatible polymer enhances the *in vitro* and *in vivo* transfection efficiency of HVJ envelope vector. J Gene Med 2005;7:888 – 97.

25. Hosseinkhani H, Aoyama T, Ogawa O, Tabata Y. Ultrasound enhancement of *in vitro* transfection of plasmid DNA by a cationized gelatin. J Drug Target 2002;10:193 – 204.

26. Hosseinkhani H, Aoyama T, Ogawa O, Tabata Y. Tumor targeting of gene expression through metal-coordinated conjugation with dextran. J Control Release 2003;88:297 – 312.

27. Hosseinkhani H, Aoyama T, Ogawa O, Tabata Y. Liver targeting of plasmid DNA by pullulan conjugation based on metal coordination. J Control Release 2002;83:287 – 302.

28. Shpetner H, Joly M, Hartley D, Corvera S. Potential sites of PI-3 kinase function in the endocytic pathway revealed by the PI-3 kinase inhibitor, wortmannin. J Cell Biol 1996;132:595 – 605.

29. Mir LM, Tounekti O, Orlowski S. Bleomycin: revival of an old drug. Gen Pharmacol 1996;27:745 – 8.

30. Miyata T, Yamamoto S, Sakamoto K, Morishita R, Kaneda Y. Novel immunotherapy for peritoneal dissemination of murine colon cancer with macrophage inflammatory protein-1β mediated by a tumor-specific vector, HVJ-cationic liposomes. Cancer Gene Ther 2001;8: 852 – 60.

31. Fujita F, Yamashita-Futsuki I, Eguchi S, et al. Inactivation of porcine endogenous retrovirus by human serum as a function of complement activated through the classical pathway. Hepatol Res 2003;26: 106 – 13.

32. Okada H, Wu X, Okada N. Complement-mediated cytolysis and azidothymidine are synergistic in HIV-1 suppression. Int Immunol 1998; 10:91 – 5.

33. Hirano T, Fujimoto J, Ueki T, et al. Persistent gene expression in rat liver *in vivo* by repetitive transfections using HVJ-liposome. Gene Ther 1998;5:459 – 64.

34. Buttiglieri S, Galetto A, Forno S, DeAndrea M, Matera L. Influence of drug-induced apoptotic death on processing and presentation of tumor antigens by dendritic cells. Int J Cancer 2003;106: 516 – 20.

[6] Y. Kaneda, in preparation.

35. Cao ZA, Daniel D, Hanahan D. Sub-lethal radiation enhances anti-tumor immunotherapy in a transgenic mouse model of pancreatic cancer. BMC Cancer 2002;2:11.

36. Pavlovic J, Nawrath M, Tu R, Heinicke T, Moelling K. Anti-tumor immunity is involved in the thymidine kinase-mediated killing of tumors induced by activated Ki-ras(G12V). Gene Ther 1996;3:635 – 43.

37. Kawai T, Akira S. Pathogen recognition with Toll-like receptors. Curr Opin Immunol 2005;17:1 – 7.

38. Bowie AG, Haga IR. The role of Toll-like receptors in the host response to viruses. Mol Immunol 2005;42:859 – 67.

39. Lopez CB, Garcia-Saraste A, Williams BR, Moran TM. Type I interferon induction pathway, but not released interferon, participates in the maturation of dendritic cells induced by negative-strand RNA viruses. J Infect Dis 2003;187:1126 – 36.

40. Lopez CB, Moltedo B, Alexopoulou L, Flavell RA, Moran TM. TLR-independent induction of dendritic cell maturation and adaptive immunity by negative-strand RNA virus. J Immunol 2004;173:6882 – 9.

41. Ito T, Amakawa R, Inaba M, et al. Plasmacytoid dendritic cells regulate Th cell responses through OX40 ligand and type I IFNs. J Immunol 2004;172:4253 – 9.

Construction of a novel DNA decoy that inhibits the oncogenic β-catenin/T-cell factor pathway

Yosuke Seki,[1] Hirofumi Yamamoto,[1] Chew Yee Ngan,[1] Masayoshi Yasui,[1] Naruya Tomita,[2] Kotaro Kitani,[1] Ichiro Takemasa,[1] Masataka Ikeda,[1] Mitsugu Sekimoto,[1] Nariaki Matsuura,[4] Chris Albanese,[5] Yasufumi Kaneda,[3] Richard G. Pestell,[5] and Morito Monden[1]

[1]Department of Surgery; [2]Division of Clinical Gene Therapy, Department of Geriatric Medicine; [3]Division of Gene Therapy Science, Graduate School of Medicine; [4]Department of Pathology, School of Allied Health Science, Faculty of Medicine, Osaka University, Osaka, Japan; and [5]Department of Oncology, Lombardi Comprehensive Cancer Center, Georgetown University, Washington, District of Columbia

Abstract

The oncogenic β-catenin/T-cell factor (TCF) signal is a common trigger inducing expressions of various cancer-related genes and is activated in various types of human malignancy. The aim of this study was to create an effective double-stranded DNA decoy that would interfere with endogenous TCF hyperactivity in tumor cells. We first established the TCF-activated model using nontumor human embryonic kidney 293 (HEK293) cells by introducing a β-catenin cDNA. Based on a consensus TCF-binding sequence in the cyclin D1 and c-myc promoters, several double-stranded oligodeoxynucleotides were designed and tested for their ability to inhibit TCF activity in the HEK293 model. Among them, the 18-mer oligodeoxynucleotide stably formed double-stranded DNA and efficiently inhibited TCF activity. FITC-labeled oligodeoxynucleotide was efficiently incorporated into the nucleus at 6 hours and remained within cells for up to 72 to 96 hours. When compared with scrambled oligodeoxynucleotide, we found that the 18-mer TCF decoy significantly inhibited TCF activity and promoter activities of the downstream target genes, such as *cyclin D1, c-myc*, and *matrix metalloproteinase 7* in HCT116 colon cancer cells. Reverse transcription-PCR assays indicated that mRNA expression of these genes decreased with treatment of the TCF decoy. Proliferation assay showed that the TCF decoy significantly inhibited growth of HCT116 tumor cells, but not of nontumor HEK293 cells. Our data provide evidence that the TCF decoy reduced both TCF activity and transcriptional activation of downstream target genes. Thus, this TCF decoy is potentially an efficient and nontoxic molecular targeting therapy for controlling malignant properties of cancer cells. [Mol Cancer Ther 2006;5(4):985–94]

Introduction

The Wnt signaling pathway plays a crucial role in various developmental and cellular processes. Wnt proteins bind to the frizzled receptor and stabilize β-catenin by inhibiting the activity of the serine/threonine kinase glycogen synthase kinase-3 that phosphorylates the NH_2 terminus of β-catenin, rendering it degradable by phosphorylation of its NH_2 terminus via the ubiquitin-proteasome pathway (1). Glycogen synthase kinase-3 forms a "destruction complex" that contains the *adenomatous polyposis coli* (*APC*) tumor suppressor gene product, axin, and others. β-Catenin then associates with the T-cell factor (TCF)/lymphocyte-enhancer factor transcriptional regulatory protein complex. This complex migrates to the nucleus, where it functions as a transcriptional activator (2).

Disorders of Wnt signaling are often associated with human gastrointestinal malignancies, especially colorectal cancer. Mutations of the *APC* gene and β-catenin are found in 80% and 12% of colorectal cancer cases, respectively (3, 4). The mutations of these genes inhibit the normal degradation of β-catenin, and thus are tightly linked to accumulation of β-catenin within the tumor cell cytoplasm and nucleus (2). Therefore, β-catenin/TCF–mediated transactivation is often enhanced in colorectal cancer cells.

Since 1998, several downstream targets of β-catenin/TCF–mediated transactivation have been identified. The c-*myc* oncogene was the first identified target (5). Others include cyclin D1, matrix metalloproteinase 7 (MMP7), membrane type 1 MMP, survivin, multidrug resistance gene 1, and peroxisome proliferator-activated receptor δ (PPARδ; refs. 6–11). There is now considerable evidence that these downstream genes may be involved in diverse malignant cell phenotypes, such as tumorigenicity, growth and invasive ability, antiapoptosis, and chemoresistance (12–16). Thus, it is likely that β-catenin/TCF–mediated transactivation is a common mechanism for inducing genes responsible for carcinogenesis and cancer progression.

Recent studies have shown that synthetic double-stranded oligodeoxynucleotides could be used as mimics of transcription factor binding sites (response elements) to

Received 9/26/05; revised 12/30/05; accepted 1/25/06.

Grant support: Grant-in Aid for Cancer Research from the Ministry of Education, Science, Sports, and Culture Technology, Japan (H. Yamamoto), and a grant for the third-term Comprehensive Strategy for Cancer Control from the Ministry of Health Labour and Welfare.

The costs of publication of this article were defrayed in part by the payment of page charges. This article must therefore be hereby marked advertisement in accordance with 18 U.S.C. Section 1734 solely to indicate this fact.

Requests for reprints: Hirofumi Yamamoto, Department of Surgery and Clinical Oncology, Graduate School of Medicine, Osaka University, 2-2 Yamada-oka, Suita City, 565-0871 Osaka, Japan. Phone: 81-6-6879-3251; Fax: 81-6-6879-3259. E-mail: kobunyam@surg2.med.osaka-u.ac.jp

doi:10.1158/1535-7163.MCT-05-0388

competitively bind the factors and thus inhibit transcription (17–21). In this article, we describe construction of a series of double-stranded oligodeoxynucleotides, based on a consensus sequence of the TCF response element. By transfection with sequence variant oligodeoxynucleotides, and reverse transcription-PCR (RT-PCR), we present evidence that an 18-mer oligodeoxynucleotide is optimal as a TCF decoy that is capable of inhibiting transcription of TCF and downstream target genes, thus blocking the oncogenic β-catenin/TCF pathway. To our knowledge, this is the first report of construction of a TCF decoy that efficiently inhibits the endogenous TCF activity in tumor cells.

Materials and Methods

Cell Lines

The human embryonic kidney 293 (HEK293) cell line and HCT116 colon cancer cell line were obtained from the American Type Culture Collection (Rockville, MD). They were grown in DMEM plus 10% (v/v) fetal bovine serum, 100 units/mL penicillin, and 100 μg/mL streptomycin, in 5% CO_2, at 37°C.

Transfection Reagents

The β-catenin expression vector was a generous gift from Dr. Bert Vogelstein (Johns Hopkins University School of Medicine, Baltimore, MD; ref. 2). The pcDNA3 vector was purchased from Invitrogen (Carlsbad, CA). Transfection was carried out with the expression vector (β-catenin plasmid and/or pcDNA3) using the LipofectAMINE 2000 reagent (Invitrogen) as recommended by the manufacturer.

Luciferase Reporter Assay

TCF transcriptional activity and its target gene promoter activities were determined by luciferase reporter assays. A TCF reporter plasmid kit was purchased from Upstate Biotechnology (Waltham, MA). The TOPflash transfection plasmid contains three wild-type response element (binding site) sequences for the β-catenin/TCF/lymphocyte-enhancer factor complex in each reading polarity, upstream of a minimal c-fos promoter and luciferase gene. The FOPflash plasmid is identical, except that the binding site sequences are mutated to serve as a negative control. The cyclin D1 reporter construct was previously described (6). The c-myc reporter (5) and the MMP7 reporter (7) were kindly provided by Drs. Bert Vogelstein and Thomas Brabletz (University of Erlangen-Nürnberg, Erlangen, Germany), respectively. Twenty-four hours after transfection with the reporter plasmid, HEK 293 or HCT116 cells were collected, and cell extracts were prepared using the reporter lysis buffer in the Luciferase Assay System (Promega, Madison, WI). The luciferase-mediated luminescence was measured by the Luciferase Assay System (Promega). The phosphoglycerate kinase/*luc* plasmids contain the *firefly luciferase* gene (*luc*) under control of the phosphoglycerokinase (PGK) promoter (22) was obtained from J. Miyazaki (Division of Stem Cell Regulation Research, Osaka University Graduate School of Medicine) and used as a control reference. All reporter experiments were done in triplicate cultures. For relative luciferase activity, light units were adjusted to the mean of the control group, which was then corrected at relative value of 1.0. Accordingly, all values are calculated and represented as mean-adjusted value. Error bar indicated deviation from the mean adjusted value.

RT-PCR

Total cellular RNA was extracted using TRIzol reagent (Life Technologies, Inc., Gaithersburg, MD). RT-PCR was done as we previously described (23, 24). Briefly, cDNA was generated from 1 μg RNA with avian myeloblastosis virus reverse transcriptase (Promega). To minimize the influence of genomic DNA contamination in the RT-PCR products, the primers were designed to span exon-intron junctions. We used *porphobilinogen deaminase* (*PBGD*; refs. 24, 25) as control for the amount of total RNA. For negative controls, samples without RNA were assayed together.

PCR amplification was done in a 25 μL reaction mixture containing 2 μL cDNA, 1× PCR buffer, 1.5 mmol/L $MgCl_2$, 0.8 mmol/L deoxynucleotide triphosphatase, 0.2 μmol/L each primer, and 1 unit Taq DNA polymerase (AmpliTaq Gold; Roche Molecular Systems, Inc., Pleasanton, CA). PCR was set up using the following protocols: one cycle of denaturing at 95°C for 12 minutes, and then (*a*) for *cyclin D1*, 30 cycles of 95°C for 1 minute, 60°C for 1 minute, and 72°C for 1 minute; (*b*) for *c-myc*, 30 cycles of 95°C for 1 minute and 65°C for 1 minute, and 72°C for 1 minute; (*c*) for *MMP7*, 35 cycles of 95°C for 1 minute, 55°C for 1 minute, and 72°C for 1 minute; (*d*) for *PPARδ*, 35 cycles of 95°C for 1 minute, 60°C for 1 minute, and 72°C for 1 minute; and (*e*) for *PBGD*, 40 cycles of 95°C for 1 minute, 62°C for 1 minute, and 72°C for 1 minute. All PCRs were completed with a final extension at 72°C for 10 minutes and the products were electrophoresed through 2% agarose gels stained with ethidium bromide. Primer sequences were as follows:

cyclin D1 sense: 5′-GCCGCAATGACCCCGCACGATTTC-3′
cyclin D1 antisense: 5′-TGCCTGGGCCCCTCAGATGTCCACACGT-3′
c-myc sense: 5′-TCCAGCTTGTACCTGCAGGATCTGA-3′
c-myc antisense: 5′-CCTCCAGCAGAAGGTGATCCAGACT-3′
MMP7 sense: 5′-GCAGCTATGCGACTCACCG-3′
MMP7 antisense: 5′-CTGCCTGAAGTTTCTATTTC-3′
PPARδ sense: 5′-CTTCCAGCAGCTACACAGACC-3′
PPARδ antisense: 5′-TCTGCCTGCCACAATGTCTCG-3′
PBGD sense: 5′-TGTCTGGTAACGGCAATGCGGCTGCAAC-3′
PBGD antisense: 5′-TCAATGTTGCCACCACACTGTCCGTCT-3′

Immunocytochemistry

Cells were fixed in 10% formalin for 10 minutes and 70% ethanol for 30 minutes. Immunostaining was done using a Vectastain ABC peroxidase kit (Vector Laboratories, Burlingame, CA), as we described previously (26). Slides

were incubated with mouse anti-human β-catenin monoclonal antibody (Transduction Laboratories, Lexington, KY) at a dilution of 1:1,000 for 1 hour at room temperature. Nonimmunized mouse IgG (Vector Laboratories) or PBS alone was used as a substitute for the primary antibody in the negative controls.

Synthesis of Double-Stranded Oligodeoxynucleotides

The phosphorothioate oligodeoxynucleotides and FITC-oligodeoxynucleotide conjugates were synthesized and purified by Sigma Genosys (Cambridge, United Kingdom). To prepare double-stranded oligodeoxynucleotides, sense and antisense oligodeoxynucleotides were dissolved in annealing buffer [10 mmol/L Tris (pH 7.5–8.0), 50 mmol/L NaCl, and 1 mmol/L EDTA] at a concentration of 100 μmol/L. Each sense-antisense pair was annealed by heating at 95°C for 10 minutes. The reaction mixture was then allowed to cool to room temperature and stored at 4°C.

Transfection of Double-Stranded Oligodeoxynucleotide into Cells

HEK293 and HCT116 cells were counted by hemacytometer, plated at the appropriate numbers in six-well plates, and grown for 24 hours in the standard medium (2 mL/well) at 37°C in 5% CO_2. The medium was removed, and the cells were covered with a mixture of the Lipofect-AMINE 2000 reagent (10 μL/plate; Invitrogen) and double-stranded oligodeoxynucleotide and/or plasmid in 1 mL serum-free DMEM, and then incubated at 37°C and 5% CO_2 for 6 hours. Following this incubation, 1 mL DMEM with 10% fetal bovine serum was added to each well, bringing the fetal bovine serum concentration to 5% v/v.

Electrophoretic Mobility Shift Assay

The binding of activated TCF and sequence of the TCF response element was evaluated with TCF-electrophoretic mobility shift assay kit (Panomics, Redwood City, CA). Activated TCF was prepared as nuclear cell extracts from HCT116 cells. Binding reactions were done for 30 minutes at room temperature in mixtures of 5 μg extracted protein, 1.5 pmol biotin-labeled TCF binding probe plus 7 pmol scrambled or decoy oligodeoxynucleotide. The products were run on 6% native polyacrylamide gels, visualized by ECL detection system.

Cell Growth Assay

Twelve hours after transfection, cells were harvested and then seeded at 4,000 cells per 100 μL medium into 96-well plates. Cell growth was determined using WST-1 assay kit (Dojindo Laboratories, Co., Kumamoto, Japan; ref. 27) at indicated time point after transfection. This assay is based on mitochondrial conversion of WST-1 to yellowish formazan, being indicative of the number of viable cells. Briefly, 10 μL WST-1 reagent [2-(4-iodophenyl)-3-(4-nitrophenyl)-5-(2-disulfophenyl)-2*H*-tetrazolium, monosodium salt] was added to each well, incubated for 2 hours at 37°C. Absorbance was measured at 450 nm with a microplate reader. Cells were refed with fresh medium every 2 days.

Statistical Analysis

Data are expressed as mean ± SD. Differences between two groups were examined by the unpaired *t* test. Differences among three groups were examined by one-factor ANOVA method, followed by Tukey-Kramer multiple comparison test. A P value of <0.05 was considered statistically significant. All analyses were done using StatView 5.0 software (SAS Institute, Inc., Cary, NC).

Results

Model of β-Catenin Activation Using Nontumor HEK293 Cells

To produce the model that represents solely *β-catenin* gene activation, we introduced an expression plasmid encoding the β-catenin cDNA into nontumor HEK293 cells. This cell line originally had only little β-catenin expression and transfection of the β-catenin plasmid–increased β-catenin expression in the nucleus (Fig. 1A, *top* and *bottom left*), whereas HCT116 colon cancer cells exhibited strong β-catenin expression in both the cytoplasm and nucleus (Fig. 1A, *top right*). When the concentration of β-catenin plasmid was increased, TCF activity, as well as promoter activities of the target genes, *cyclin D1*, *c-myc*, and *MMP7* concordantly increased (Fig. 1B and C). The expression of mRNAs for *cyclin D1*, *c-myc*, *PPARδ*, and *MMP7* also increased after transfection with the β-catenin expression plasmid (Fig. 1D). These experiments and subsequent assays were repeated at least twice and reproducible results were obtained.

Consensus Sequence of TCF Binding Site in the β-Catenin Target Gene Promoters and Design of DNA Decoys

GCTTTGATC is the consensus sequence of TCF binding sites commonly found in the cyclin D1 (GG*GCTTTG-ATC*TTT) and c-myc (GC*GCTTTGATC*AAG) promoters (5, 6). The consensus TCF-binding site mapped at 25 bp 5′ of the cyclic AMP-responsive element binding protein–binding site within the *cyclin D1* promoter (6). The TCF decoy was designed from this sequence. A six-nucleotide subsequence (*CTTTGA*) occurs in the promoter of the *MMP7* gene (ATC*CTTTGA*AAGAC or GAA*CTTTGA*AAGTA; ref. 8). Likewise, the promoter for PPARδ has six or eight nucleotides in common with this consensus sequence (TGT*CTTTG*TACTCG or TG*GCTTTCATC*TGA; ref. 12). To search for candidate oligodeoxynucleotides that are capable of maximally inhibiting TCF activity, we designed a series of oligodeoxynucleotide decoy constructs of various lengths, as well as negative-control oligodeoxynucleotides with two base replacements (Fig. 2A). This strategy was based on the hypothetical competition between the decoy and target gene sequences for binding the endogenous β-catenin/TCF complex (Fig. 2B). Using HEK293 cells activated to produce β-catenin, we found that cells treated with 0.1 μmol/L oligodeoxynucleotide decoys of 14- to 18-mer, exhibited large reductions in TCF transcription compared with cells treated with oligodeoxynucleotide decoys of 6-, 9-, or 12-mer (Fig. 3A). SDS-PAGE revealed that the 18-mer oligodeoxynucleotide decoy formed a stable double-strand structure (Fig. 3B), whereas the sense and antisense sequences of the 14-mer DNA decoy easily separated after storage (data not shown). In cells treated with the 18-mer

oligodeoxynucleotide decoy at 0.1 μmol/L, promoter activities of the genes for TCF, cyclin D1, c-myc, and MMP7 were largely inhibited (Fig. 3C). On the other hand, the TCF decoy did not affect PGK-driven luciferase expression.

Incorporation of FITC-Conjugated Double-Stranded DNA into HEK293 and HCT116

To determine the transfection efficiency and subcellular localization of the TCF decoy, we traced FITC-conjugated TCF decoy under the fluorescence microscopy. After transfection, the labeled decoy was internalized as early as 1 hour and it was detected in almost all of the cells at 6 hours in both HEK293 and HCT116 cells (Fig. 4A and B). Confocal laser microscopy survey revealed incorporation of decoy into the nucleus (Fig. 4B). A time course study indicated that the labeled decoy gradually degraded but still detectable in the nucleus for

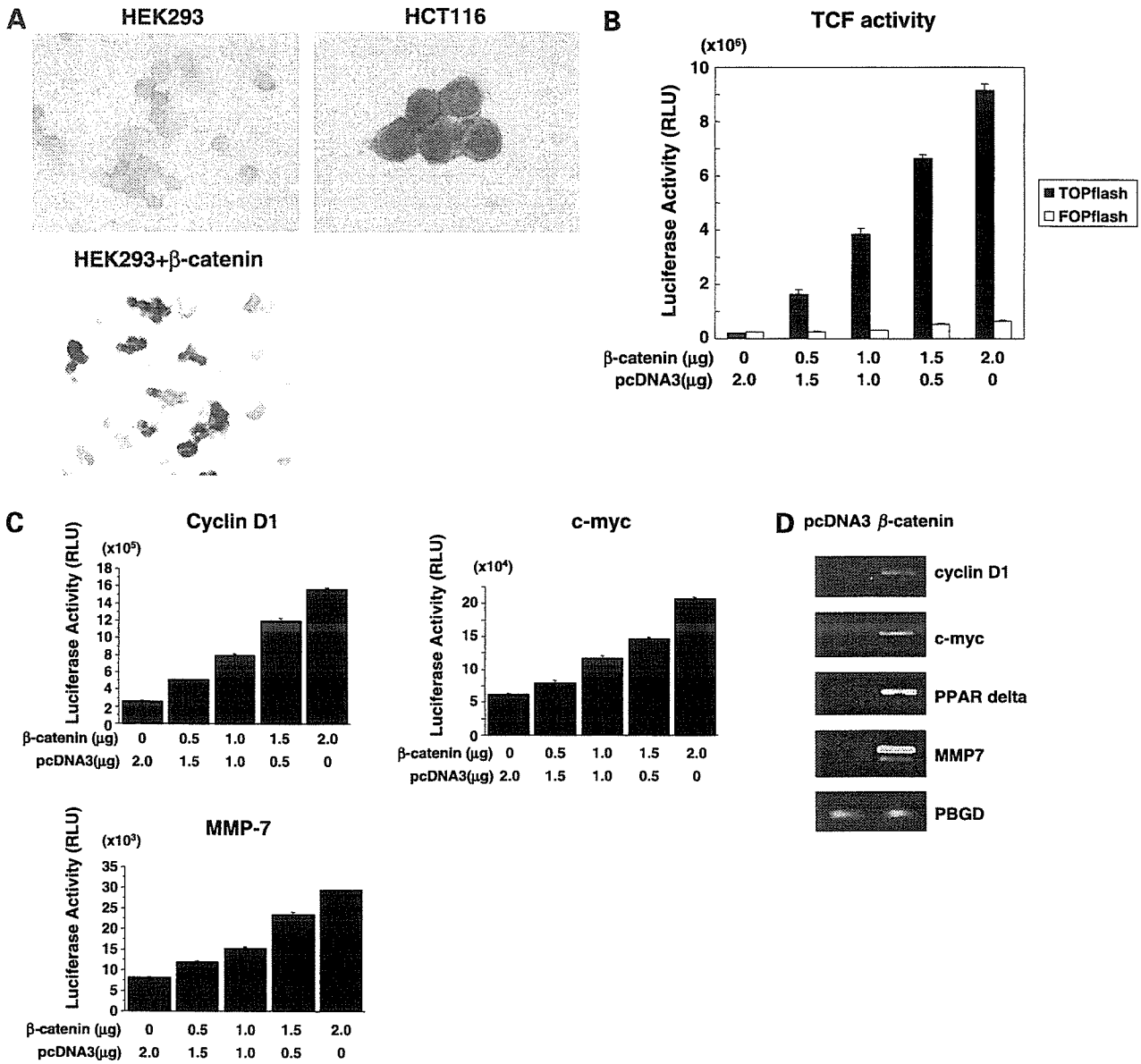

Figure 1. **A,** immunocytochemistry for β-catenin. HEK293 cells were stained with the anti-β-catenin antibody 48 h after transfection with either 1 μg pcDNA3 (*top left*) or μg β-catenin plasmid (*bottom left*). β-catenin expression in HCT116 colon cancer cells (*top right*). Magnifications, ×100. **B,** TCF activities. Transfection with the β-catenin plasmid enhanced TCF activity dose dependently in HEK293 cells when assayed using TOPflash reporter plasmid (0.5 μg). The TOPflash plasmid (0.5 μg) served as a negative control. pcDNA3 plasmid was used to adjust DNA quantity. *Columns,* mean of triplicate cultures; *bars,* SD. **C,** promoter activities of cyclin D1, c-myc, and MMP7 induced by β-catenin plasmid. **D,** mRNA expression of β-catenin target genes determined by RT-PCR, when HEK293 cells were transfected with 1 μg of either pcDNA3 (*left*) and β-catenin plasmid (*right*). *PBGD*, a housekeeping gene, served as an internal control.